NATIONAL ADVISORY COMMITTEE FOR AERONAUTICS

TECHNICAL NOTE 2429

STUDY OF VORTEX SHEDDING AS RELATED TO SELF-EXCITED TORSIONAL OSCILLATIONS OF AN AIRFOIL

By Raymond L. Chuan and Richard J. Magnus

California Institute of Technology

Washington

September 1951

NATIONAL ADVISORY COMMITTEE FOR AERONAUTICS

TECHNICAL NOTE 2429

STUDY OF VORTEX SHEDDING AS RELATED TO SELF-EXCITED TORSIONAL OSCILLATIONS OF AN AIRFOIL

By Raymond L. Chuan and Richard J. Magnus

SUMMARY

This report covers the results of the experimental investigation of the self-excited torsional oscillation of an NACA 0006 airfoil suspended elastically. The relationship between the torsional oscillation and the shedding of vortices was investigated for this airfoil.

Two types of oscillation phenomena were found in the investigation. One type, exhibited by cases with angles of attack just above stall, persisted with increasing velocity without reaching any apparent limit within the range of velocity attainable in the present wind tunnel. The other type, exhibited by cases with higher angles of attack, only showed self-excited oscillations in a certain range of velocity, the range decreasing with increasing angle of attack.

INTRODUCTION

The investigation of the failure of the Tacoma Narrows Bridge in 1941 indicated that an elastically suspended flat plate exposed at moderate angle of attack to a wind stream exhibited self-excited torsional oscillations of considerable amplitude. An investigation to study this phenomenon further was subsequently undertaken at the Guggenheim Aeronautical Laboratory, California Institute of Technology, under the sponsorship and with the financial assistance of the National Advisory Committee for Aeronautics.

Unpublished work at the California Institute of Technology has covered test results of bending oscillations and preliminary work on torsional oscillations. Reference 1 deals with torsional oscillations only and indicates that additional research is necessary to investigate the mechanism for the starting of the self-excited torsional oscillations as related to the shedding of vortices. Reference 1 also indicates that there was no upper limit to the range of velocities in which the oscillations occurred. The present investigation shows that for angles of

attack beyond a certain limit there are upper limits to the velocities at which self-excited oscillations occur. The results of reference 1 indicate that the amplitude of the oscillations depends on past history. Therefore, in the present research program the airfoil was allowed to start from rest every time the velocity was varied. The study of the vortex shedding in an attempt to relate it to the oscillation was performed with the aid of hot-wire anemometers.

SYMBOLS

α	geometric angle of attack of airfoil when stationary, degrees
V	wind velocity, feet per second
V_1	lower critical velocity at which oscillation starts, feet per second
V_2	upper critical velocity at which oscillation no longer starts, feet per second
V_3	velocity at which maximum amplitude occurs, feet per second
θ	amplitude of oscillation, degrees
θ_{max}	maximum amplitude of oscillation at a given angle of attack, degrees
n	frequency of oscillation, cycles per second
N	frequency of vortex shedding with stationary airfoil, cycles per second
N_1	N corresponding to V_1, cycles per second
N_2	N corresponding to V_2, cycles per second
N_3	N corresponding to V_3, cycles per second
b	airfoil chord, feet
K	dimensionless Von Kármán number
q_o	free-stream dynamic pressure
ΔH	difference in total head of free stream and wake

DESCRIPTION OF APPARATUS

An open-return wind tunnel, as shown schematically in figure 1, was used for this research program. To insure that the oscillations were not caused by any fluctuation in the flow through the test section, three screens were placed at the entry of the contraction section. Two of these were made of cheese cloth, and the third was made of 20-mesh copper screen. They were spaced at 1-foot intervals. A 1-inch gap was left between the diffuser section and the fan section to prevent any oscillation of the engine-propeller section from being transmitted to the working section.

The suspension system consisted of a 24S-T Duralumin rod mounted on each end of the airfoil as shown in figure 2. This allowed maximum freedom for torsional oscillation while affording little freedom for any other mode of motion. Two sets of rods were used in this experiment. With the suspended mass constant, the frequency of oscillation of the airfoil depends on the diameter of the rods. One set of Duralumin rods of 0.188-inch diameter (designated suspension 1) was used to obtain a torsional frequency of approximately 12 cycles per second and another set of 0.25-inch diameter (designated suspension 2) was used to obtain a frequency of approximately 20 cycles per second.

The NACA 0006 airfoil was of laminated wood construction with a 9-inch chord and 41-inch span. Each end of the airfoil was fitted with two Duralumin blocks into which fitted the pins that connected the airfoil to the suspension system. The details of the suspension system are shown in figure 2.

The linear relation of stress and strain of the torsion rods furnished a convenient means of measuring both the frequency and the amplitude of the oscillations by the use of a strain gage mounted on one of the suspension rods at an angle of 45° to the axis of the rod. Thus, the deflection of the strain gage was directly proportional to the angle of twist. The output of the strain gage was fed through a 6-channel amplifier designed for both strain-gage and hot-wire measurements. The current through the strain gage, supplied by a 12-volt direct-current source, was approximately 10 milliamperes. The method of calibration used here was such that the fluctuation in the voltage across the strain gage or in the gain of the amplifier could not affect the measurement of the angular deflections. This was accomplished by shunting the strain gage with any one of several precision resistors. With a resistor shunted across the undeflected strain gage, the reduced net resistance was measured with a Wheatstone bridge. Then, the shunt was removed and the airfoil was deflected to such a position as to give the same amount of reduction in

the resistance. The angular deflection at this point was recorded. This was done with four different shunting resistors. By means of a selector switch and a microswitch any one of these four shunts could be placed across the strain gage, each shunt corresponding to a known angular deflection. The output of the amplifier was fed into a 6-channel recording oscillograph, Heiland Type A-400R6. The calibration appeared as a stepped trace on the recording paper. By comparing the height of the step and the subsequent oscillation record, the exact angular deflection could be obtained independent of any variation in the voltage across the strain gage or in the amplifier gain. The oscillograph had a timer which marked 0.01-second timing lines on the recording tape.

Two sets of hot-wire anemometers were used to measure the vortex-shedding frequency. One set was mounted fixed with respect to the tunnel, while the other was mounted on the airfoil itself and moved with it. The fixed hot-wires were mounted on faired Duralumin struts, one protruding into the wind stream from the bottom of the test section and the other from the top. Both struts were mounted on traversing mechanism permitting motions both vertical to and along the wind-stream direction. The moving hot-wires were mounted by means of rigid frames made of 1/8-inch copper tubing secured to the top surface of the airfoil. One such hot-wire was mounted near the leading edge and the other one near the trailing edge, as shown in figure 3. The anemometers were made of 1/4-mil platinum wire with a length of approximately 3/16 inch, as shown in figure 3. Approximately 100 to 150 milliamperes of current were used. The output of the hot-wires was amplified and recorded in the same manner as for the strain gage. Since the frequency of shedding was all that was needed, no calibration was necessary.

A cathode-ray oscilloscope was used in parallel with the recording oscillograph so that visual observation of both the oscillation of the airfoil and the shedding of vortices could be made while records were being taken. The best position for picking up the vortex frequency at any velocity and angle-of-attack setting was chosen by observing the output of the oscilloscope while the hot-wire was moved across the wake of the traversing mechanism. This was necessary because inside the wake it was difficult to obtain any defined pattern of flow because of high turbulence. On the border of the wake the influence of the vortex formation could be felt by the hot-wire without any appreciable effect of the wake turbulence.

The accuracy of velocity measured by means of a pitot-static tube mounted in the test section ahead of the airfoil was ±0.2 feet per second. The accuracy of setting the angle of attack with respect to the wind-stream direction was ±1/3°. The accuracy of oscillation amplitude measurement with the shunt calibrations was ±0.1°. At the lower angles of attack, from stall to about 15°, the accuracy of vortex frequency reading was approximately ±15 percent, while at higher angles it was approximately ±3 percent.

TEST PROCEDURE

The velocity survey of the working section was made by placing a pitot-static tube at 30 positions with the airfoil removed, and the results are presented in figure 4.

The wake surveys were for angles of attack of 8°, 12°, and 15°, both with the airfoil held stationary and with it oscillating. The results are presented in figures 5 to 8.

Tuft surveys were made at angles of attack of 6°, 8°, 12°, 15°, and 19°, with the airfoil stationary, and the results are presented in figure 9.

For the oscillation amplitude and the vortex shedding frequency measurements the following procedure was followed: The airfoil was mounted on suspension 1 and set at the desired angle of attack, and the velocity was increased slowly until the oscillation just started. The velocity was then decreased approximately 5 feet per second to a point where there was no longer any oscillation. With the airfoil held stationary the lower hot-wire was moved into position, and by observing the pattern on the oscilloscope the best position was found for determining the vortex frequency. A record was then taken of the vortex shedding frequency. The velocity was then increased and another vortex frequency record was taken with the airfoil stationary. The airfoil was released and allowed to begin self-excited oscillation. If there was any oscillation at that particular velocity, it was allowed to reach a steady value as indicated by the oscilloscope. When steady state was reached, the amplifier gain was adjusted so that the traces filled up the oscilloscope screen. The vertical gain in the oscilloscope was already adjusted so that full use of the screen corresponded to the full use of the recording tape in the oscillograph. Again the airfoil was stopped and a calibration mark was put in the record. One of four calibration marks, corresponding to amplitudes of approximately 1°, 3°, 7°, and 10°, could be chosen. The airfoil was then released again and allowed to reach steady-state oscillation before a record was made of the oscillation.

The airfoil was again stopped and the velocity was increased by about 1 foot per second, following which the procedure just described was repeated. This was done up to the point where oscillation no longer started; or, in cases where the oscillation amplitude kept increasing, the run was terminated when the amplitude was near the elastic limit of the torsion rods, which was about 15°. These tests were run for angles of attack of 7°, 8°, 10°, 12°, 14°, 15°, 18°, 21°, 23°, 25°, 27°, and 29°. The results of these runs are presented in figure 10.

Similar measurements were made with suspension 2, at angles of attack of 8°, 12°, and 25°. The results of these measurements are presented in figure 11.

In order to obtain a complete set of data to show the relationship between the vortex shedding frequency of the stationary airfoil and the angle of attack with velocity as a parameter, hot-wire frequency records were taken over a velocity range of about 20 to 45 feet per second for angles of attack of 7°, 8°, 10°, 12°, 14°, 15°, 18°, 21°, 23°, 25°, 27°, and 29°. Results of these runs are presented in figures 12 to 14.

By manipulating the hot-wire mounted from the top of the test section, the point of flow separation on the upper surface was found for angles of attack of 9°, 12°, 15°, 18°, and 21°. A scale was mounted over the top of the airfoil, with zero at the leading edge, so that the point of separation could be measured with respect to the leading edge. Results are presented in figure 15.

Finally, in order to study the shedding phenomenon while the airfoil was oscillating and to examine the phase relation of the shedding with the oscillation, simultaneous records of the strain gage and of the hot-wires mounted on the airfoil were taken for angles of attack of 8°, 10°, and 18°. For each angle of attack and velocity setting a record was first taken with the oscillation traces and the shedding traces from the leading edge put on the same tape so that the phase relations could be examined. For the same configuration another record was made with the oscillation traces and the shedding traces taken behind the trailing edge. Results of these tests are presented in figure 16.

EXPERIMENTAL RESULTS

The results of the velocity survey shown in figure 4 indicate that the maximum velocity variation was about 1.6 percent in the test section.

The wake surveys are presented in figures 5 to 8. Figures 5 and 6 show that the oscillating airfoil produced a wake of nearly the same width as the stationary one. A comparison of figure 7 with figure 8 indicates that the wake for 12° of angle of attack was wider than that for 15°.

The tuft surveys, as presented in figure 9, show that the flow was not strictly two-dimensional.

Figure 10 gives the results of the oscillation amplitude and the shedding frequency as a function of velocity for angles of attack of 7°, 8°, 10°, 12°, 14°; 15°, 18°, 21°, 23°, 25°, 27°, and 29°, using

suspension 1, which had a frequency of approximately 12 cycles per second. These results show that for angles of attack below 14° there was apparently no upper limit of velocity at which self-excited oscillations occurred. For angles of attack higher than 14° there were upper limits, and the range of velocity in which oscillations started became less as the angle of attack was increased. It may also be seen that for the higher angles of attack the vortex-shedding frequency within the oscillation range was near the natural frequency of the oscillating system.

The plots of velocity range in which self-excited oscillation occurred as a function of angle of attack are given in figure 17. The plots of vortex frequency range in which oscillation occurred as a function of angle of attack are given in figure 18. The maximum amplitude of oscillation and the corresponding velocity and vortex frequency for the stationary airfoil as a function of angle of attack are given in figure 19. Oscillation amplitudes as a function of angle of attack with the velocity as a parameter are plotted in figure 20.

A thorough study of the oscillation phenomena using suspension 2 was not made, although limited results were obtained and are presented in figure 11. The limited velocity range of the wind tunnel restricted the scope of the investigation using the stiffer suspension.

Figure 12 gives vortex frequency of the stationary airfoil as a function of velocity for angles of attack of 7°, 8°, 23°, 27°, and 29°. This figure shows that the frequencies are quite irregular just above stall, but are regular for the higher angles.

Figures 13 and 14 show vortex shedding frequency as a function of $\sin \alpha$ at different velocities. It is seen that, instead of following a linear relation $\frac{Nb \sin \alpha}{V} = K$ as indicated by Tyler's formula given in reference 2, the shedding frequency decreases at lower angles of attack. At the higher angles the value of K ranges between 0.112 and 0.178, which is in fair agreement with the values given in reference 2. Tyler gives an average value for K of 0.15 for airfoils, while Blenk, Fuchs, and Liebers give an average value of 0.21.

Results of the measurement of point of separation are given in figure 15, which shows that the separation point on the upper surface is fixed for the range of angles of attack from stall to 14° and shifts to a new fixed position at angles of attack from 15° on.

The results with the hot-wires attached to the oscillating airfoil and measuring shedding and oscillation simultaneously are given in figure 16. These results are discussed in detail in the next section.

DISCUSSION

The factors affecting the oscillation of a system like the airfoil used in this experiment are the following: The moment of inertia of the entire system, the torsional rigidity of the suspension system, the aerodynamic damping moment, and the torsional moment caused by the vortex shedding. The moment of inertia of the system is constant if the system is at rest, but is increased by an "additional apparent moment of inertia" when it is in motion in a fluid. When the airfoil itself is assumed to be very rigid compared with the torsion rods, which is true in this case, the torsional rigidity of the system depends on the rigidity of the torsion rods, and is therefore constant. The aerodynamic damping on an oscillating airfoil depends on the angle of attack, the frequency and amplitude of oscillation, and the velocity of the air stream. Glauert shows in reference 3 that for an oscillating lifting wing this damping moment is positive except for suspension points farther forward than the 25-percent-chord point.

If the airfoil is initially at rest, energy must be put into the system to set it into oscillation. The mechanism which puts energy into the system is the periodic shedding of vortices. Experimental results show that no oscillation occurred for angles of attack less than 6°. Investigation with the hot-wire also showed that there was no shedding of vortices for angles of attack less than 6°. The lift curve for the NACA 0006 airfoil in figure 21 shows that the curve begins to deviate from a straight line after 6°. The amount of energy put in must balance the dissipation due to damping in order to maintain the oscillation. It may be expected that the energy input due to the shedding of vortices would be a maximum when the shedding frequency is equal to the oscillation frequency. At this point, if the dissipation due to damping is less than the energy input, oscillation would occur and maintain itself. However, it is conceivable that at a particular angle of attack of the airfoil and a particular velocity when the shedding frequency equals the natural frequency of the system the energy input is not sufficient, because of the low velocity, to start any oscillation. It may be seen from figure 13 that for an angle of attack of 8° the velocity at which the shedding frequency equals 12 is very low, and figure 10(b) shows that there was no oscillation at this point. At higher angles of attack, a shedding frequency of 12 requires a higher velocity, which may be sufficient to start an oscillation. Results at the higher angles of attack, as presented in figures 10(e) to 10(l), show that oscillations start when the ratio of shedding frequency to natural frequency is near one. If the velocity is increased it may be expected that the shedding frequency increases and becomes out of phase with the natural frequency, while the damping moment, at the same time, is increased because of the increase in velocity, so that oscillation will no longer start. Results given in figures 10(e) to 10(l) show this to be the case.

The results at the lower angles of attack, as given in figures 10(a) to 10(d), show that there was no upper limit to the range of velocity in which self-excited oscillation occurred, even when the shedding frequency with the stationary airfoil was as high as four times the natural frequency. Once the oscillation began it rapidly built up to very high amplitudes. This leads one to the conjecture that at these lower angles of attack the shedding frequency, once the oscillation is started, is controlled by the oscillation frequency itself, and no longer by the velocity and the stationary angle of attack. Furthermore, it is obvious that at the lower angles of attack the airfoil must go into the unstalled state during part of the cycle of oscillation. If an airfoil is stalled and unstalled periodically, the change in the circulation and, consequently, in the shedding of vortices must also be periodic and have the same frequency as the oscillation. To show that this was the case at the lower angles of attack, hot-wires were mounted on the oscillating airfoil to study the flow condition over the airfoil during the oscillation. Figure 16 shows the results of this study.

Figure 16(a) shows two traces, the sinusoidal one being the oscillation of the airfoil and the other one the flow condition over the airfoil just behind the leading edge. The amplitude of oscillation in this case was 6.5°, so that at the upper end of the travel the airfoil was at an angle of attack of 14.5° and at the lower end of the travel it was at 1.5°. It is seen that the trace of the hot-wire response from point 1 to point 2 is straight and level. Point 1 corresponds to an angular position of 1.5° and point 2 corresponds to 13.5°. Thus, the record indicates that between angular positions of 1.5° and 13.5° the flow over the airfoil was smooth. But at point 2 the smooth flow broke down sharply, indicating the shedding of a vortex. This vortex formation began just before the airfoil started on its downward swing. Figure 16(b), which gives the traces of the oscillation and the flow condition behind the trailing edge, indicates that at point 1 the flow at the trailing edge took a sudden increase in speed because of the shedding of the vortex. Thus it is seen that one vortex each was shed from the leading and trailing edges during each cycle of oscillation. Therefore, in the case of lower angle of attack, when during part of the cycle the airfoil was in the unstalled state, the oscillation frequency controlled the shedding frequency. The shedding of the vortices in turn maintained the oscillation, since the moment produced by the shedding was in phase with the oscillation. These results substantiate the statement that the oscillating airfoil must control the vortex frequency over a very large range of velocities.

At the higher angles of attack the airfoil was apparently stalled throughout the cycle of oscillation, as indicated by results given in figure 16(d), which shows the oscillation and flow condition over the airfoil at an angle of attack of 18° and oscillation amplitude of 7.0°. Figure 16(c) shows an intermediary case, in which the unstalled region was less extended than in the case represented by figure 16(a).

CONCLUDING REMARKS

At the higher angles of attack the oscillation was controlled by the shedding of vortices, and resonance between vortex shedding and oscillation was apparent. The oscillation phenomena at the lower angles of attack need to be further investigated. The exciting moments and the damping moments should be examined quantitatively in order to arrive at a more definite correlation of vortex shedding to torsional oscillations.

California Institute of Technology
Pasadena, Calif., May 25, 1948

REFERENCES

1. Levy, Charles N.: Self-Excited Torsional Oscillations of an Airfoil. Thesis, C.I.T., June 1945.

2. Fluid Motion Panel of the Aeronautical Research Committee and Others (S. Goldstein, ed.): Modern Developments in Fluid Dynamics. Vol. II The Clarendon Press (Oxford), 1938, ch. XIII, sec. 255.

3. Glauert, H.: The Force and Moment on an Oscillating Aerofoil. R. & M. No. 1242, British A.R.C., 1929.

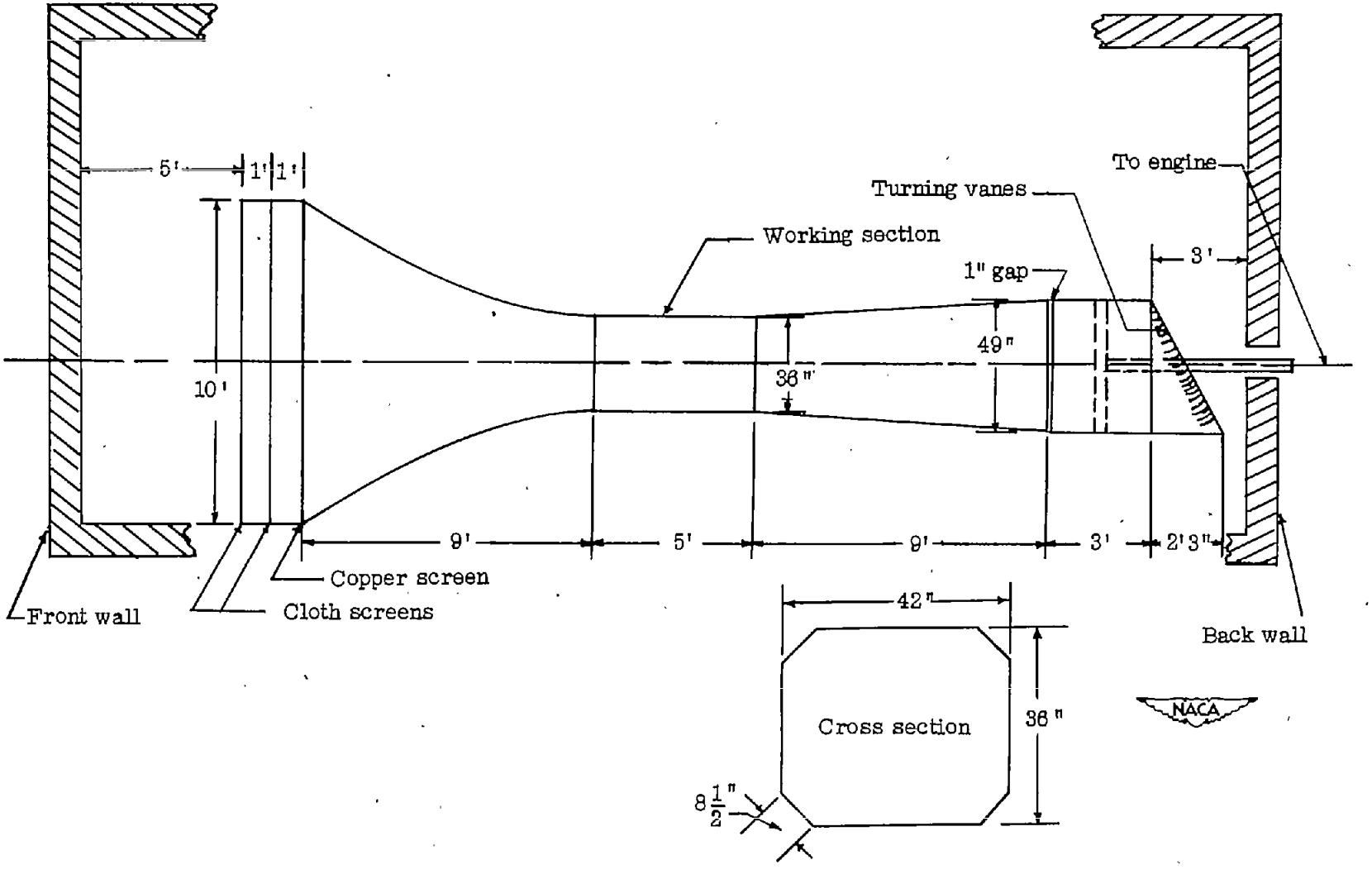

Figure 1.- Schematic sketch of open-return wind tunnel.

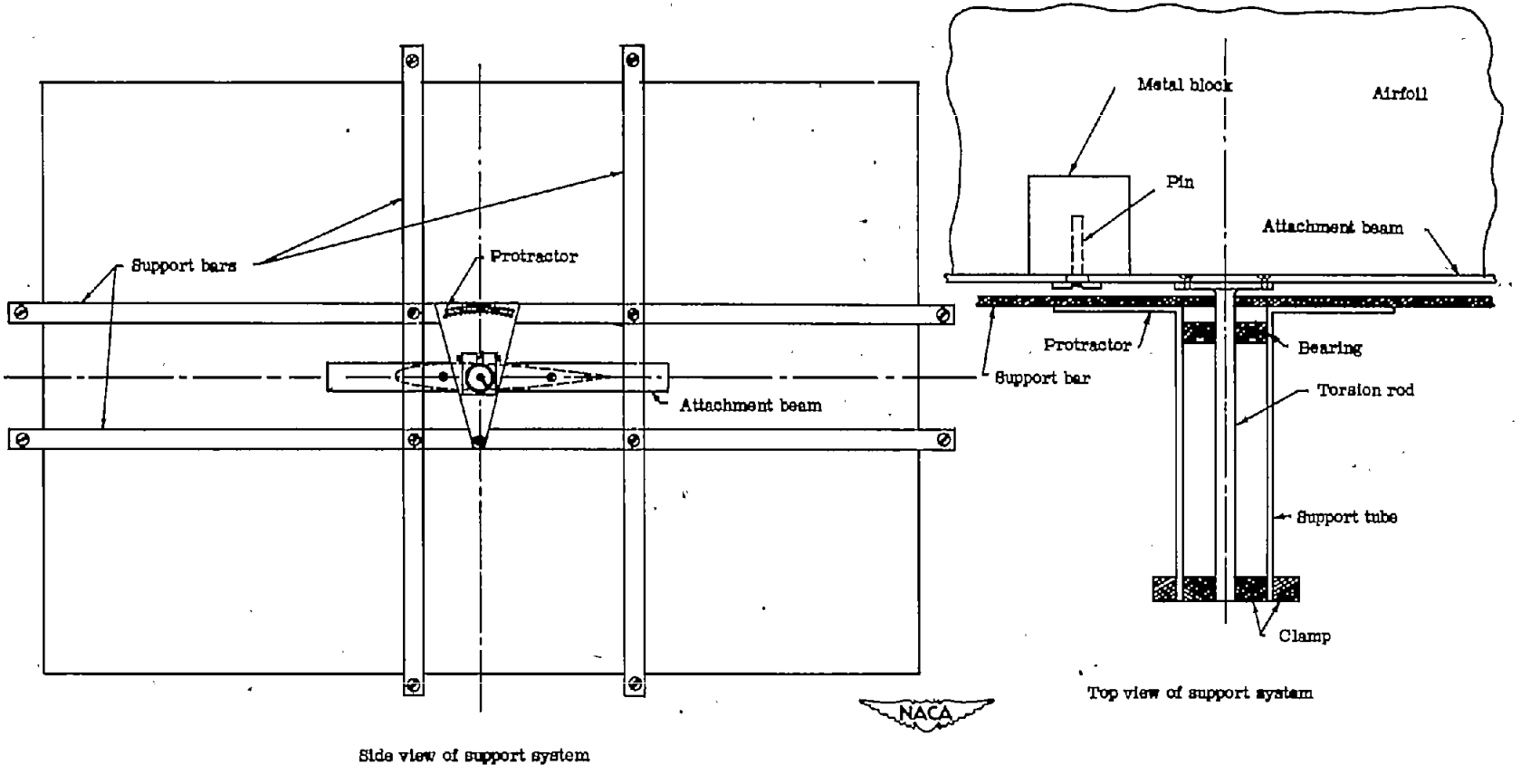

Figure 2.- Torsional oscillation suspension system.

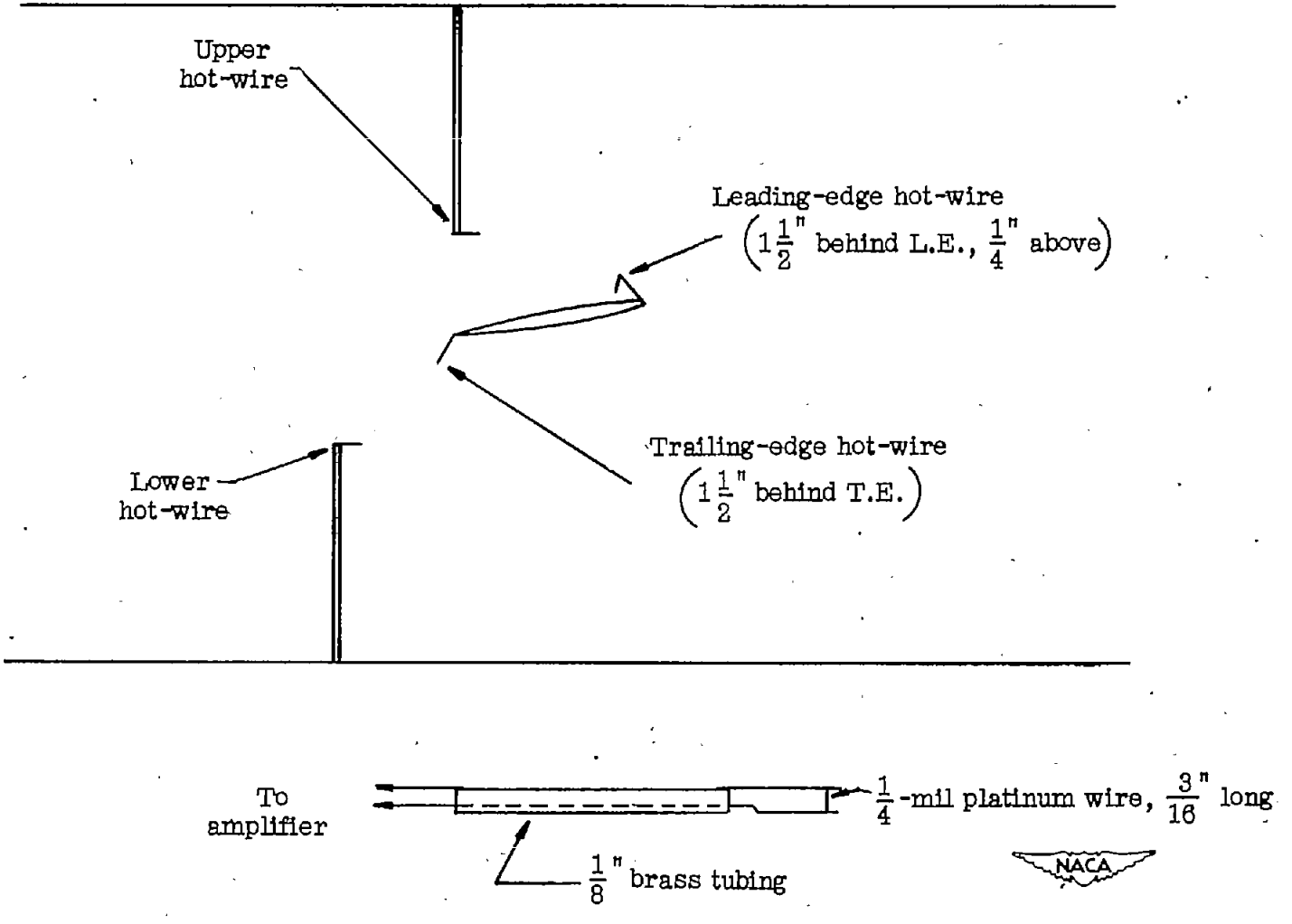

Figure 3.- Sketch of hot-wire anemometer and positions of mounted hot-wires.

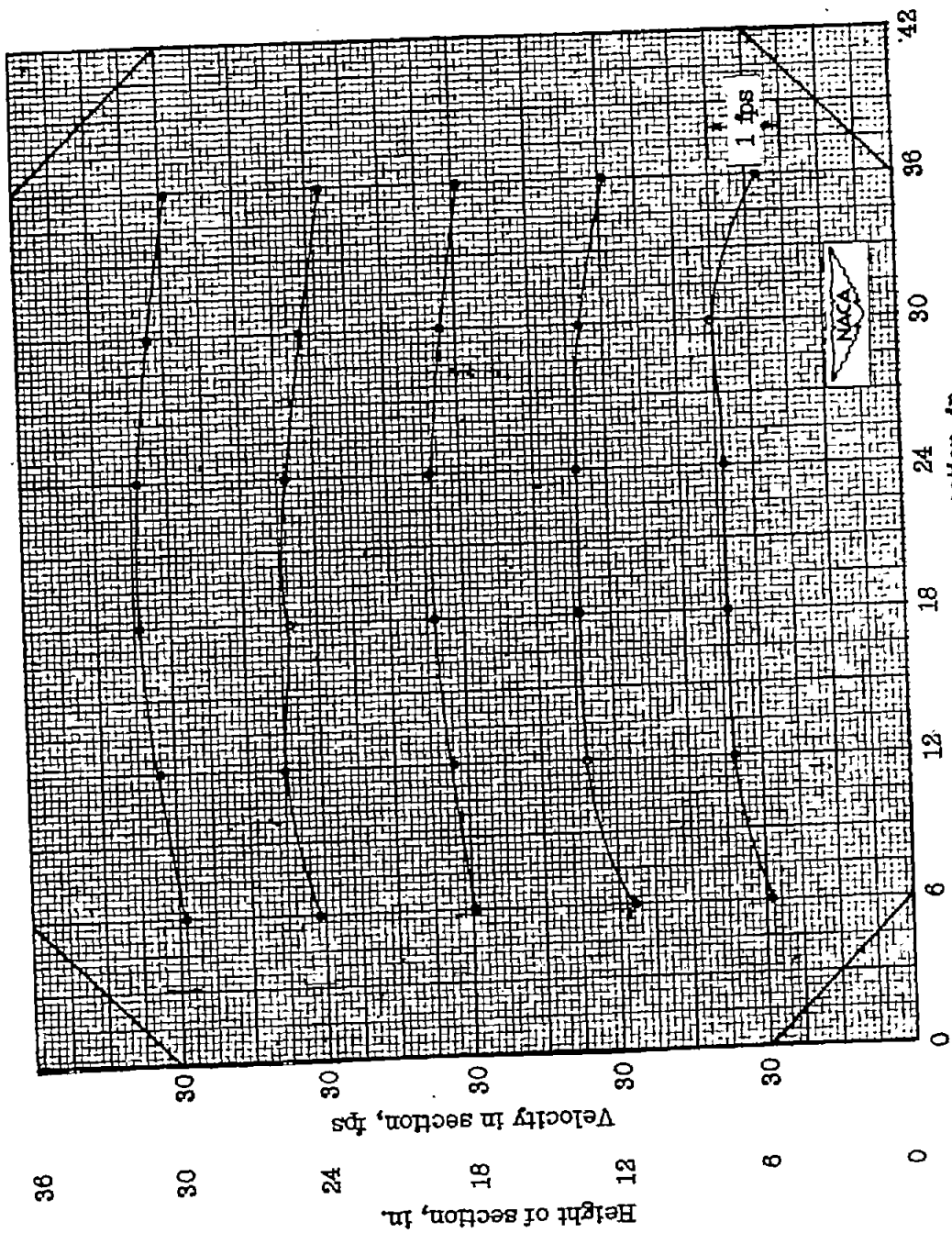

Figure 4.- Velocity survey of working section; V = 30 feet per second.

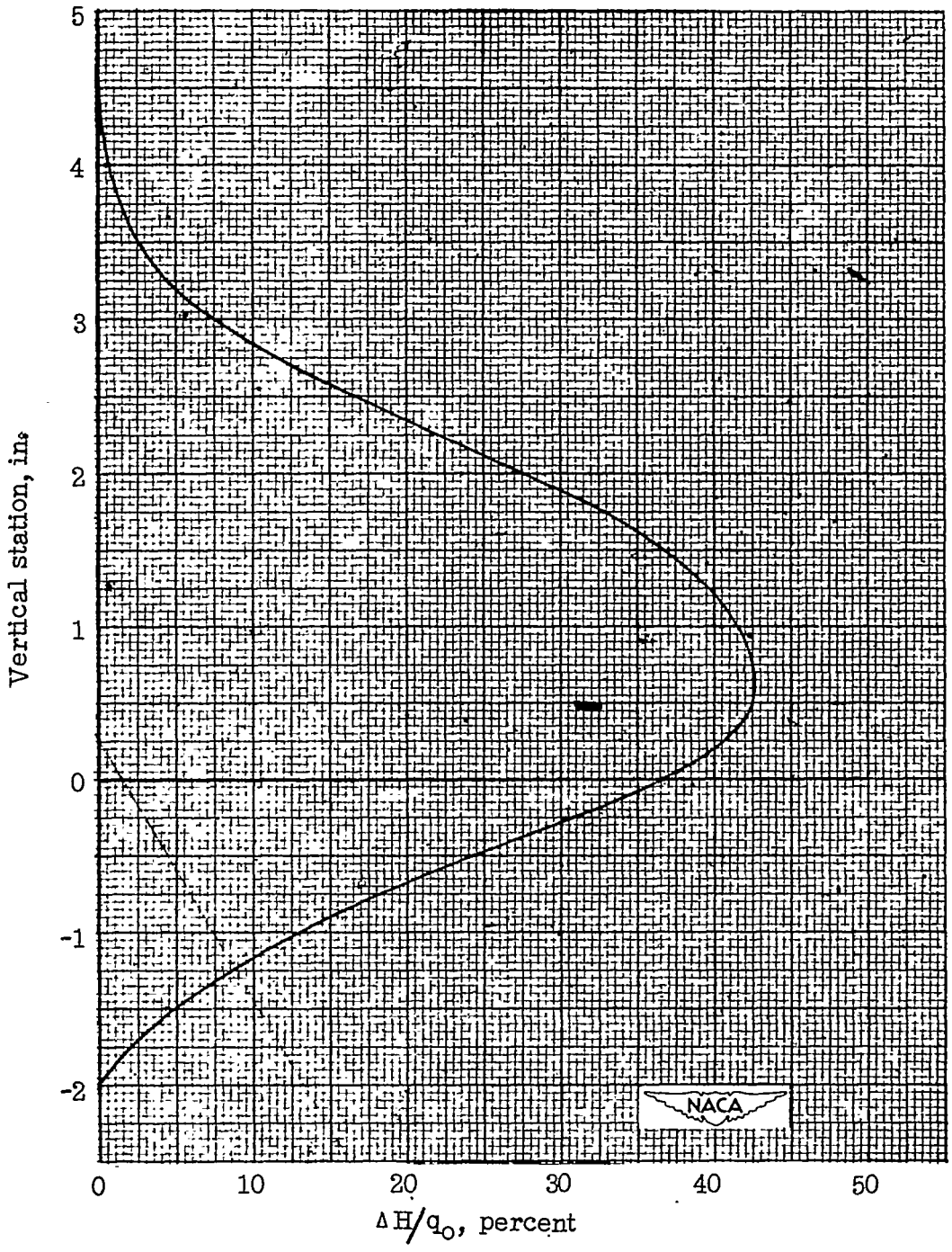

Figure 5.- Wake survey 1 chord downstream from trailing edge. No oscillation; $\alpha = 8^\circ$; V = 25.6 miles per hour.

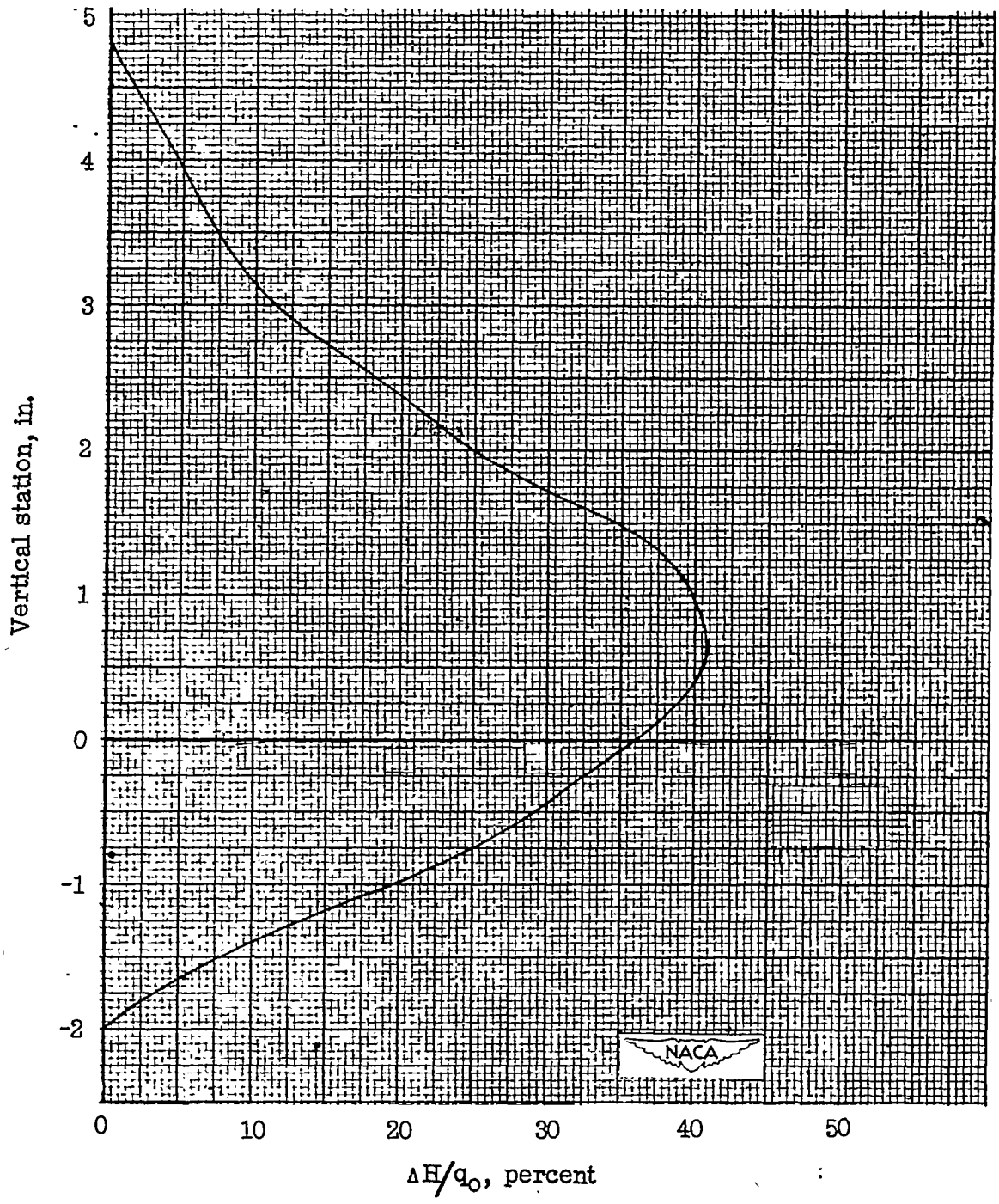

Figure 6.- Wake survey 1 chord downstream from trailing edge. Oscillating airfoil; $\alpha = 8^{\circ}$; V = 25.6 miles per hour.

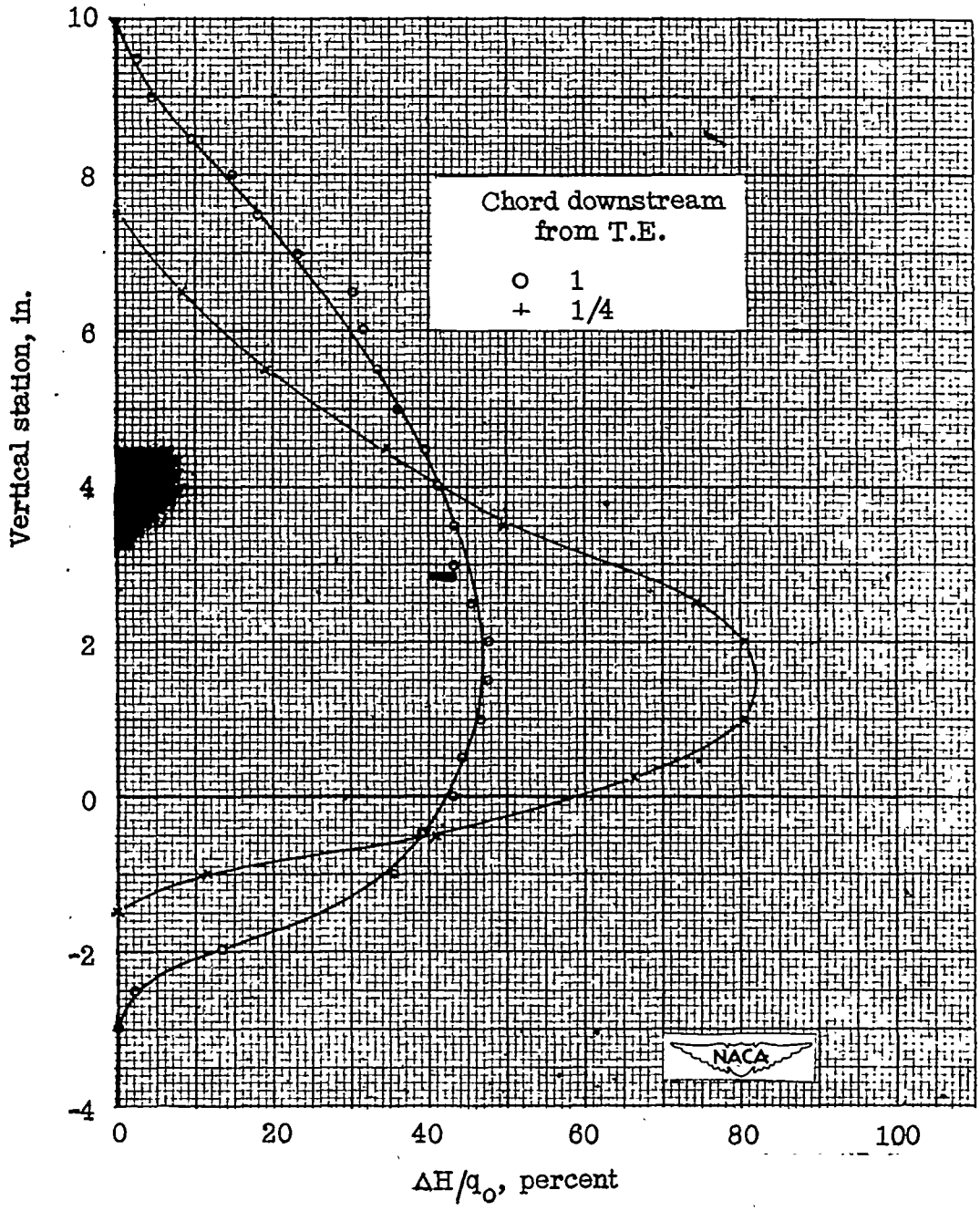

Figure 7.- Wake survey at various distances from trailing edge. Oscillating airfoil; $\alpha = 12^{\circ}$; V = 24.8 miles per hour.

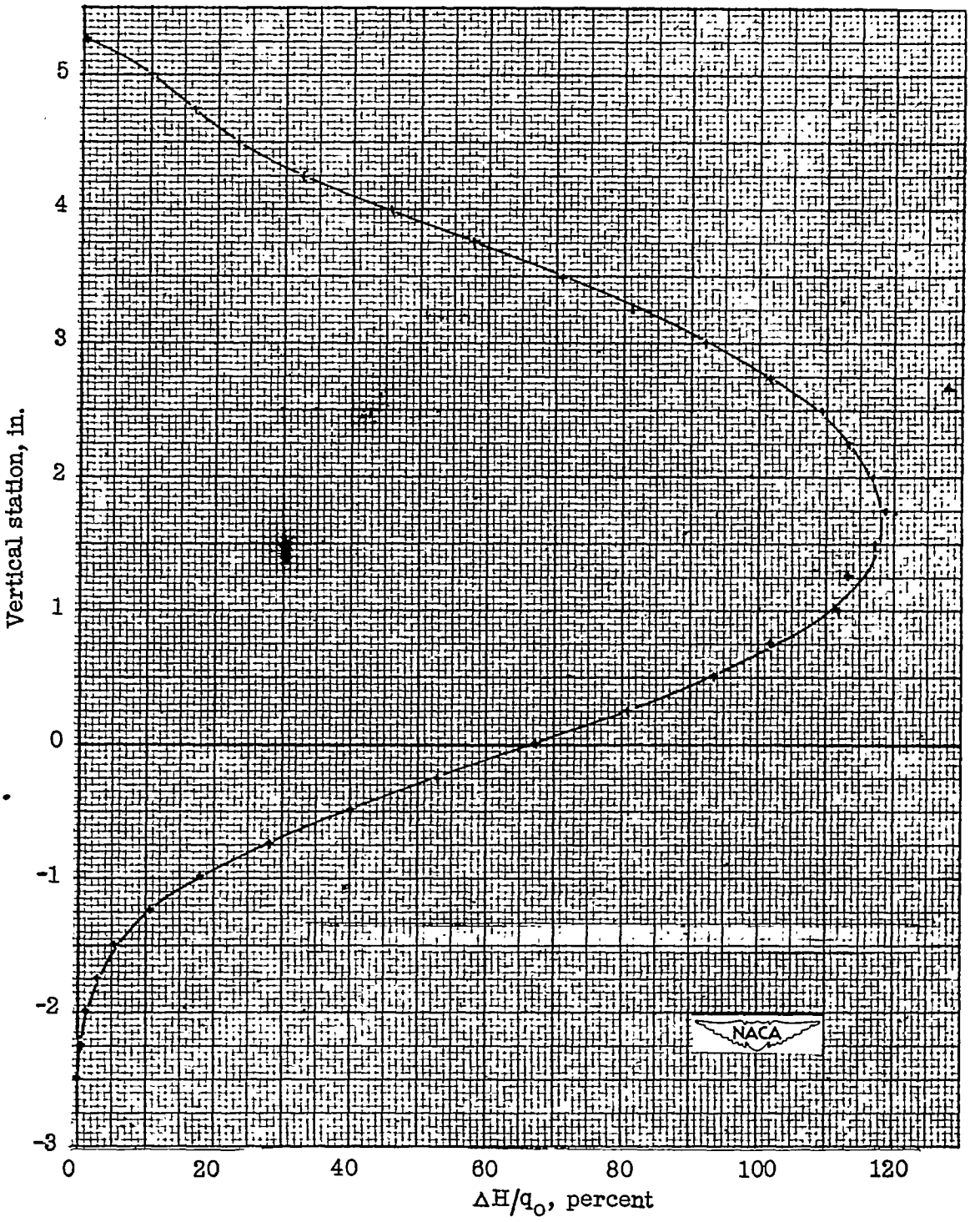

Figure 8.- Wake survey 1 chord downstream from trailing edge. Oscillating airfoil; $\alpha = 15^{\circ}$; V = 25.0 miles per hour. Instrument reading taken in very fluctuating region.

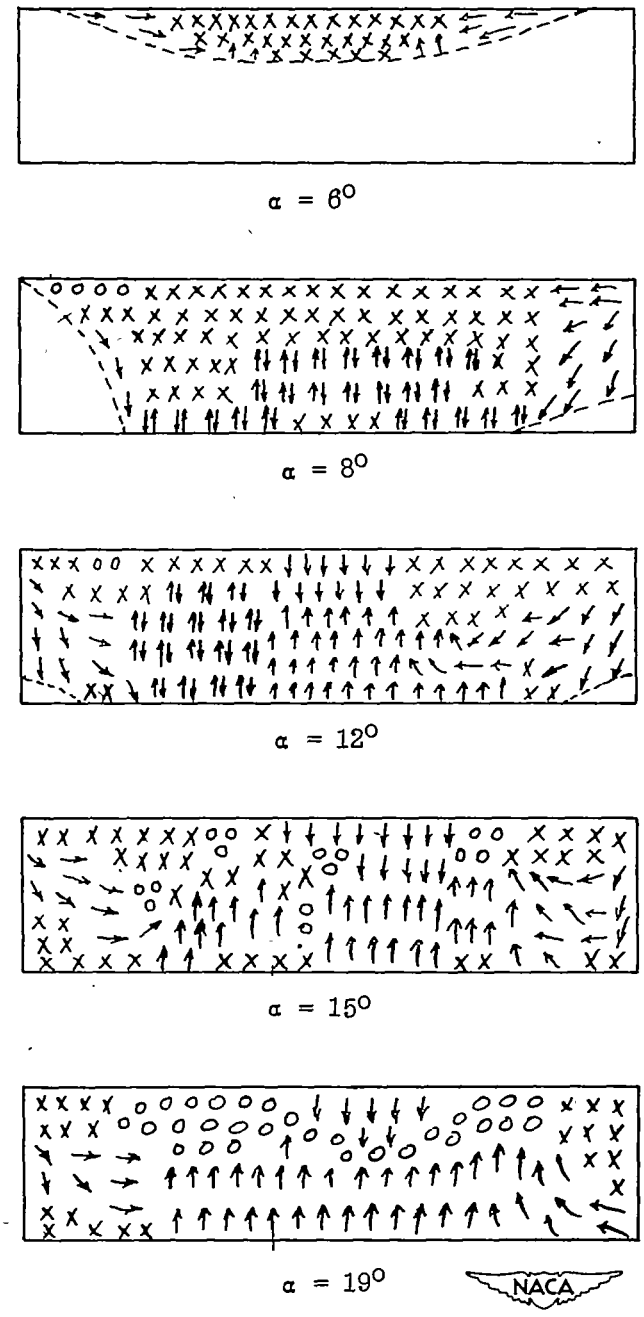

Figure 9.- Tuft surveys made at various angles of attack with airfoil held stationary. Stream direction is downward.

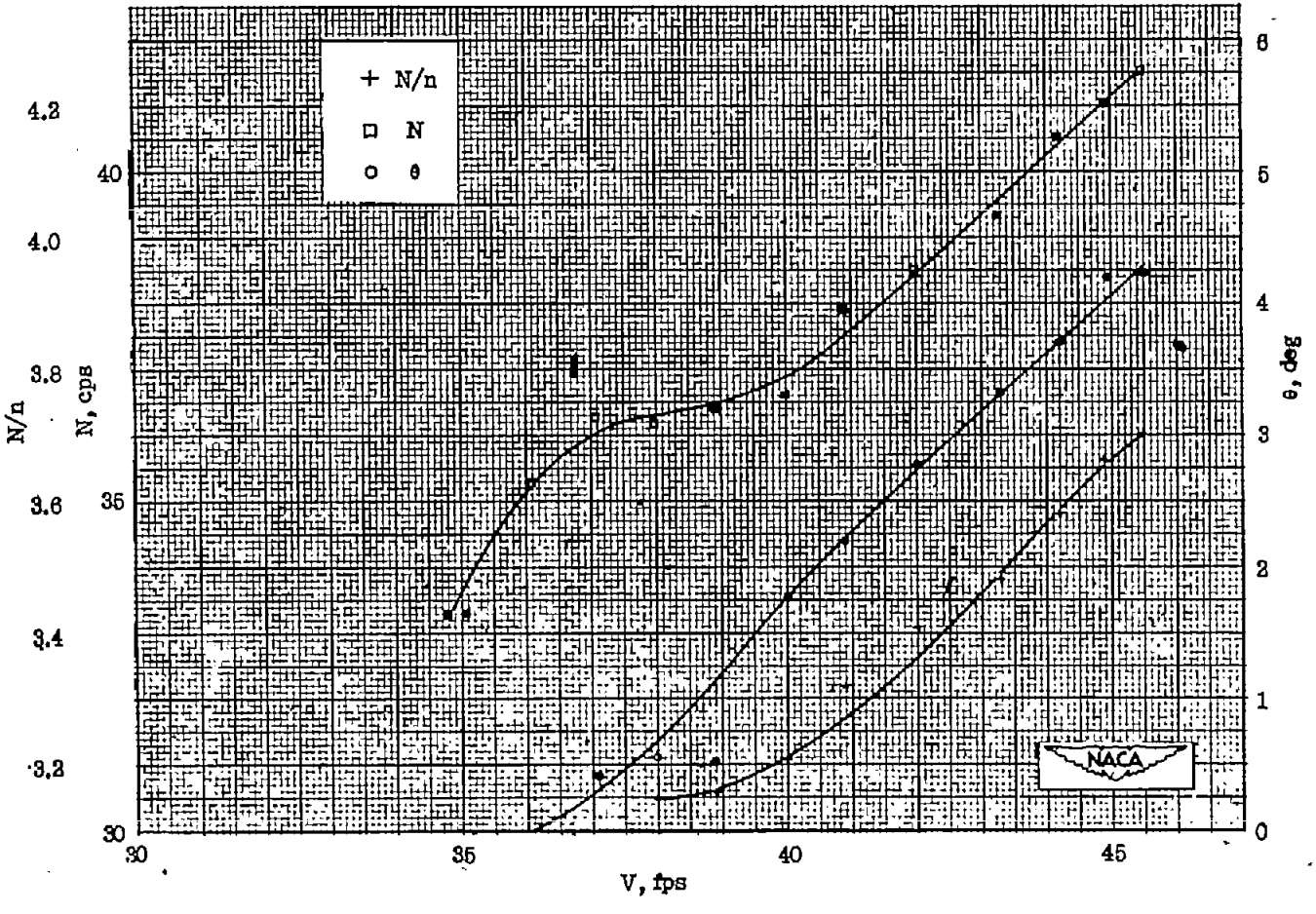

(a) $\alpha = 7^{\circ}$.

Figure 10.- Oscillation amplitude and vortex shedding frequency measurements made with suspension 1.

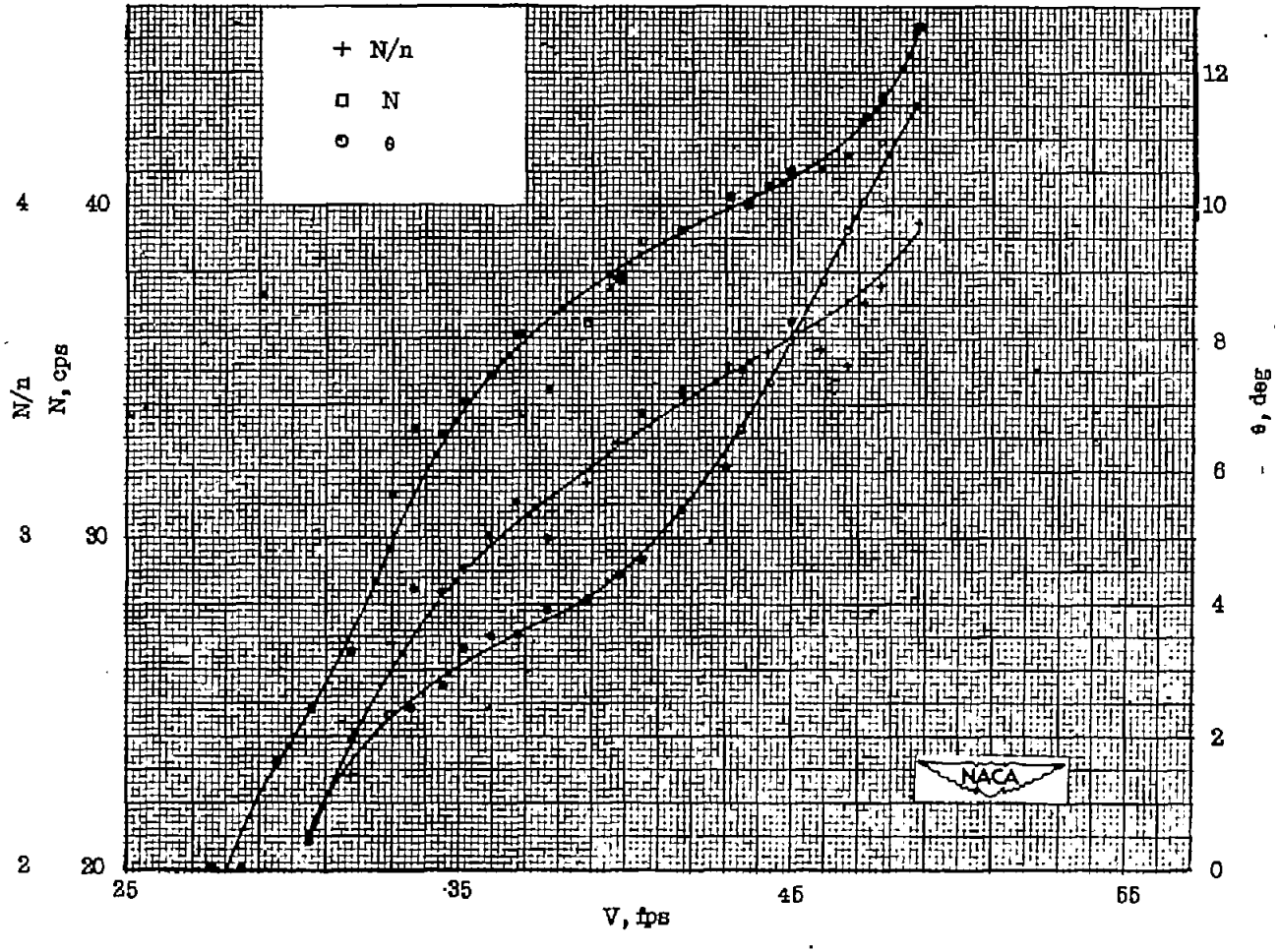

(b) $\alpha = 8^{\circ}$.

Figure 10.- Continued.

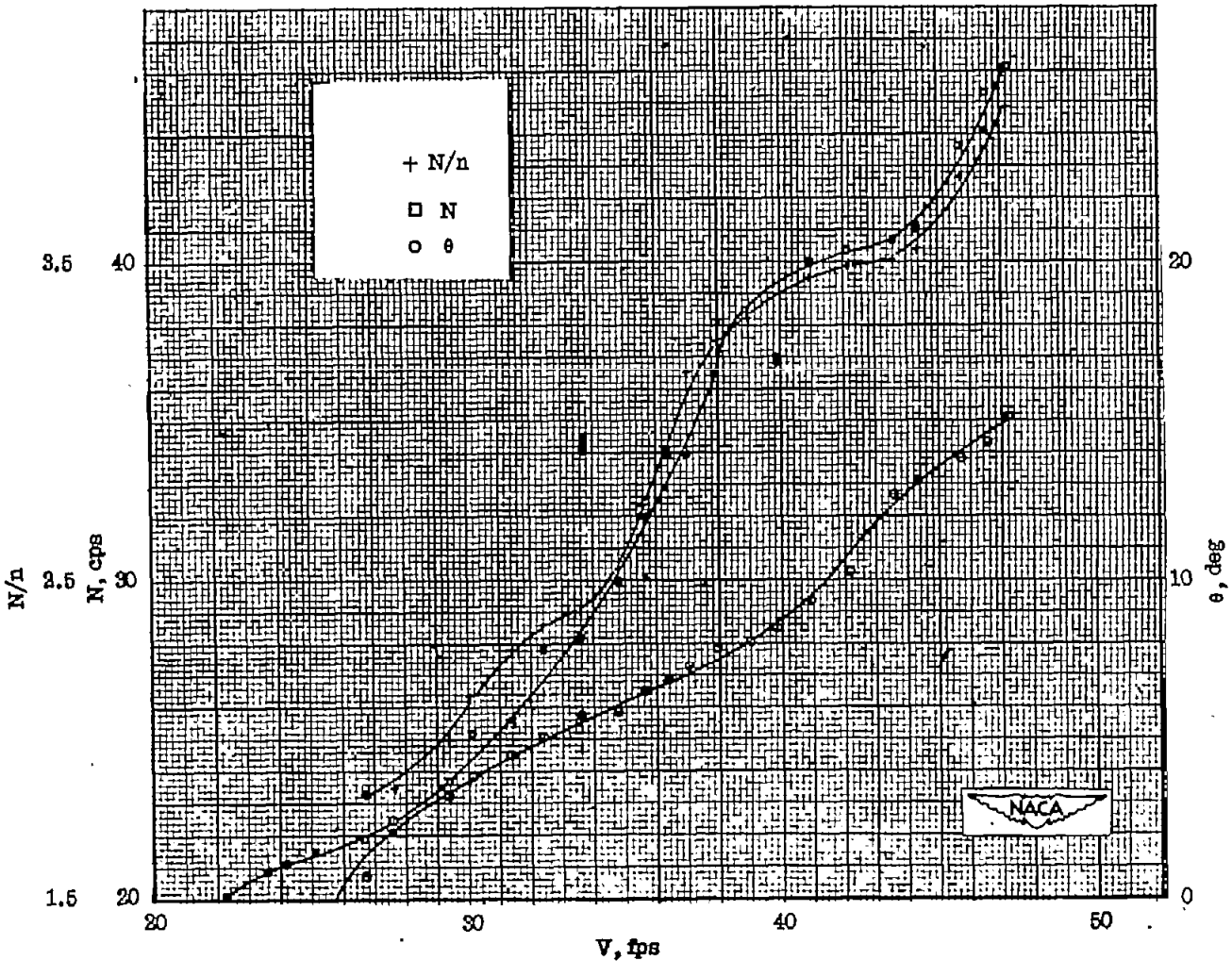

(c) $\alpha = 10^{\circ}$.

Figure 10.- Continued.

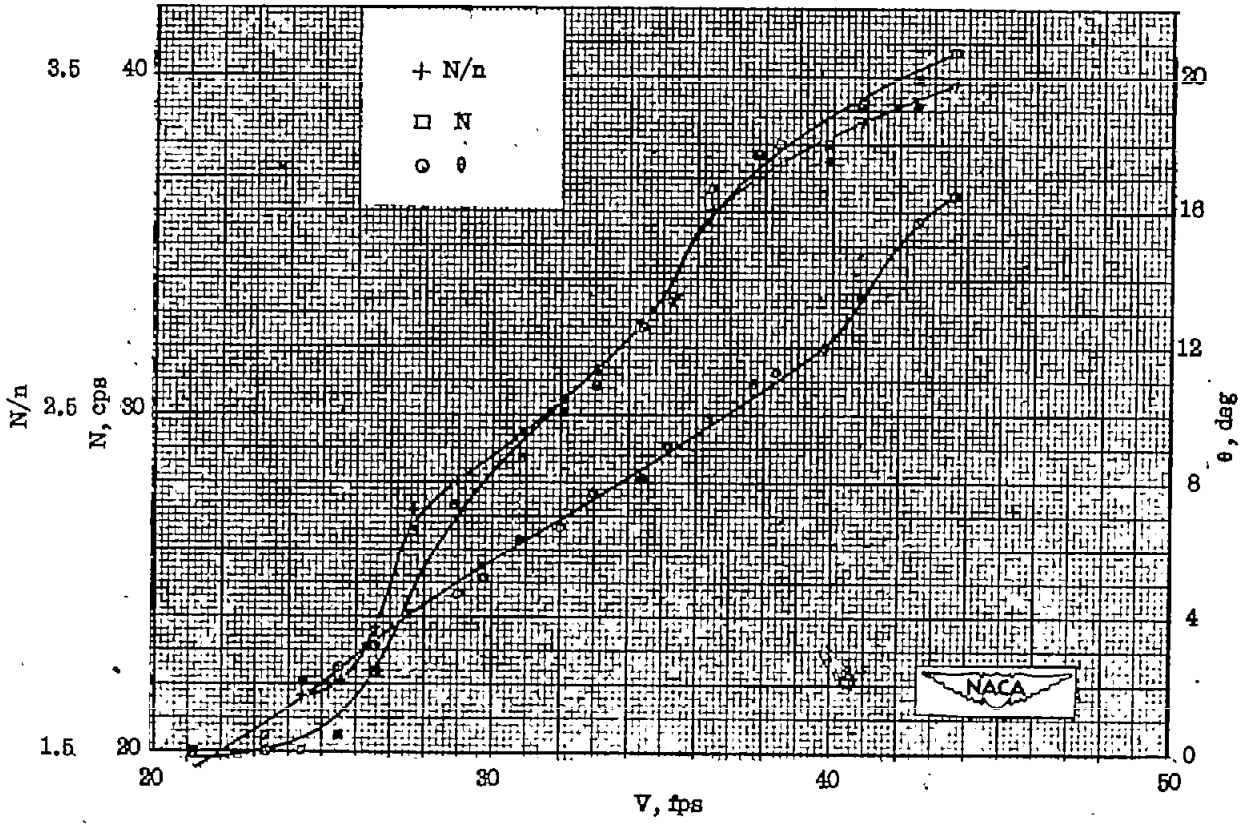

(d) $\alpha = 12^{\circ}$.

Figure 10.- Continued.

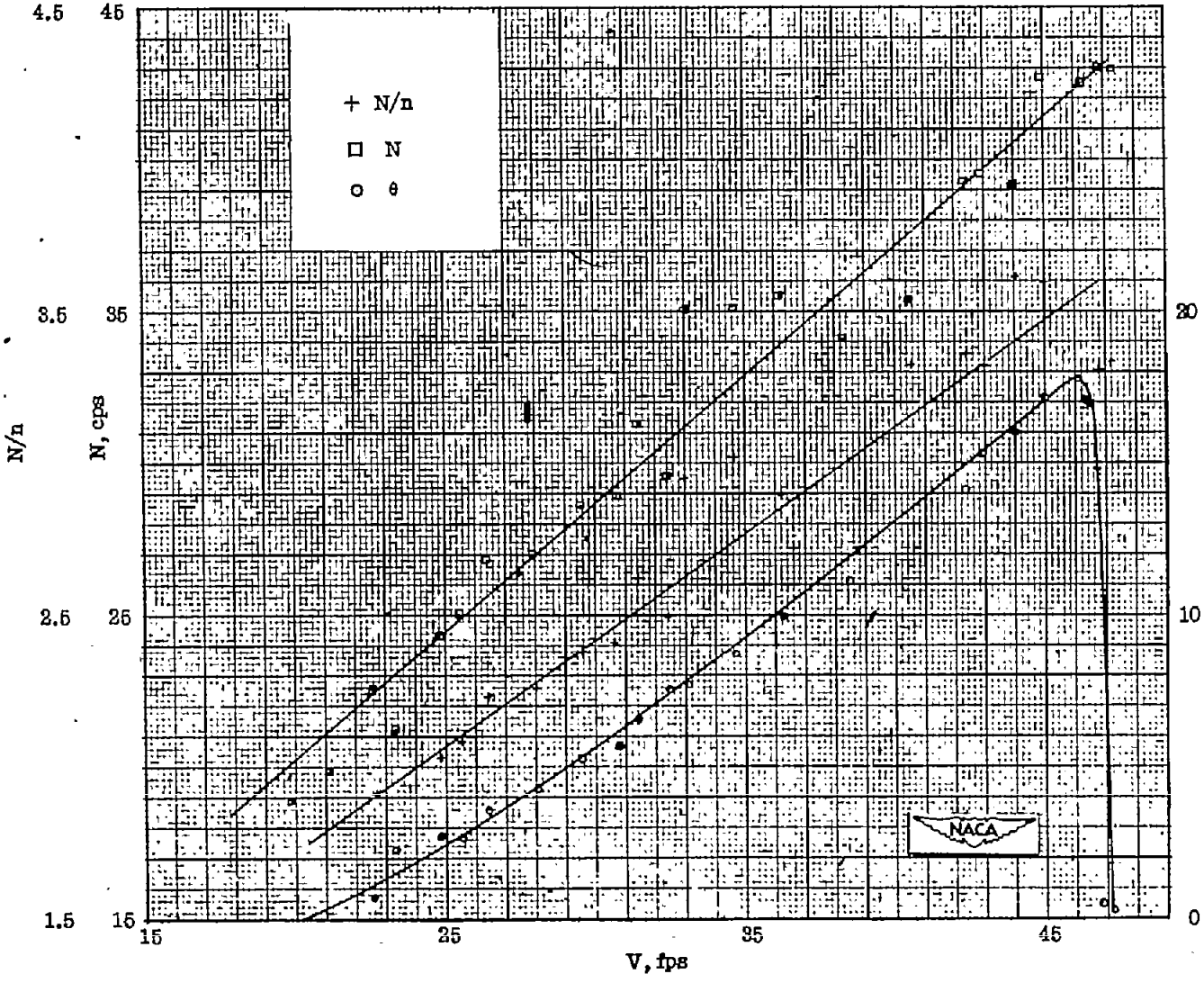

(e) $\alpha = 14^{\circ}$.

Figure 10.- Continued.

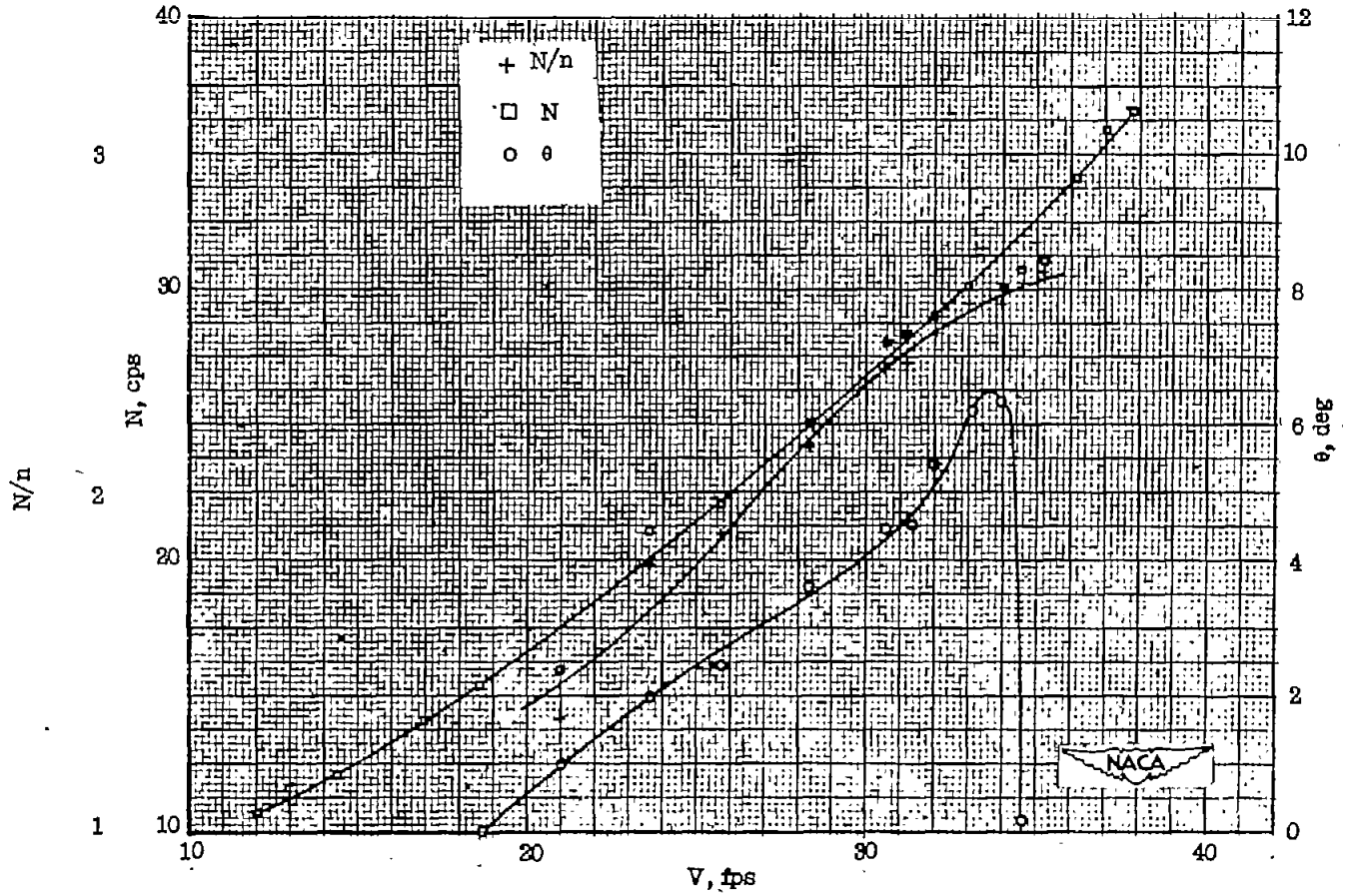

(f) $\alpha = 15^{\circ}$.

Figure 10.- Continued.

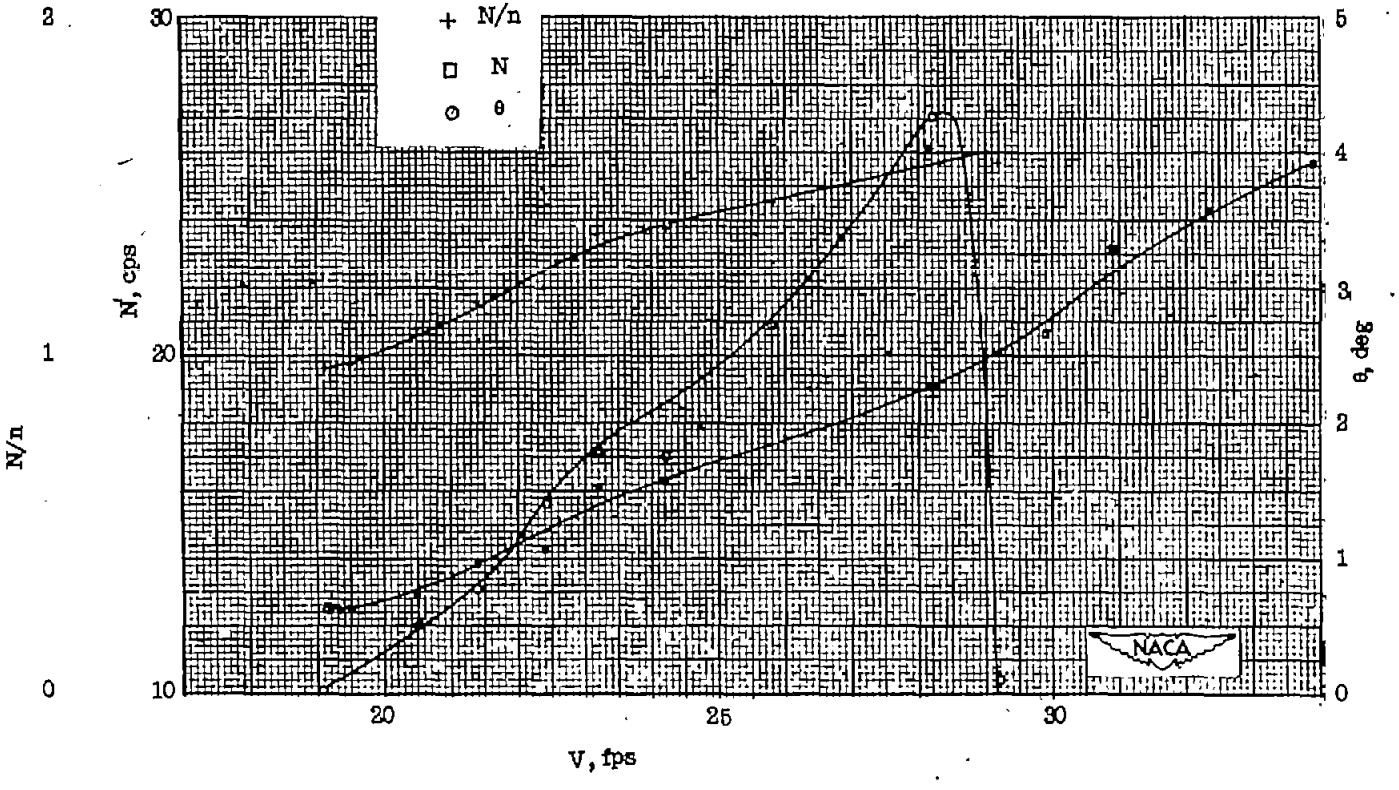

(g) $\alpha = 18^{\circ}$.

Figure 10.- Continued.

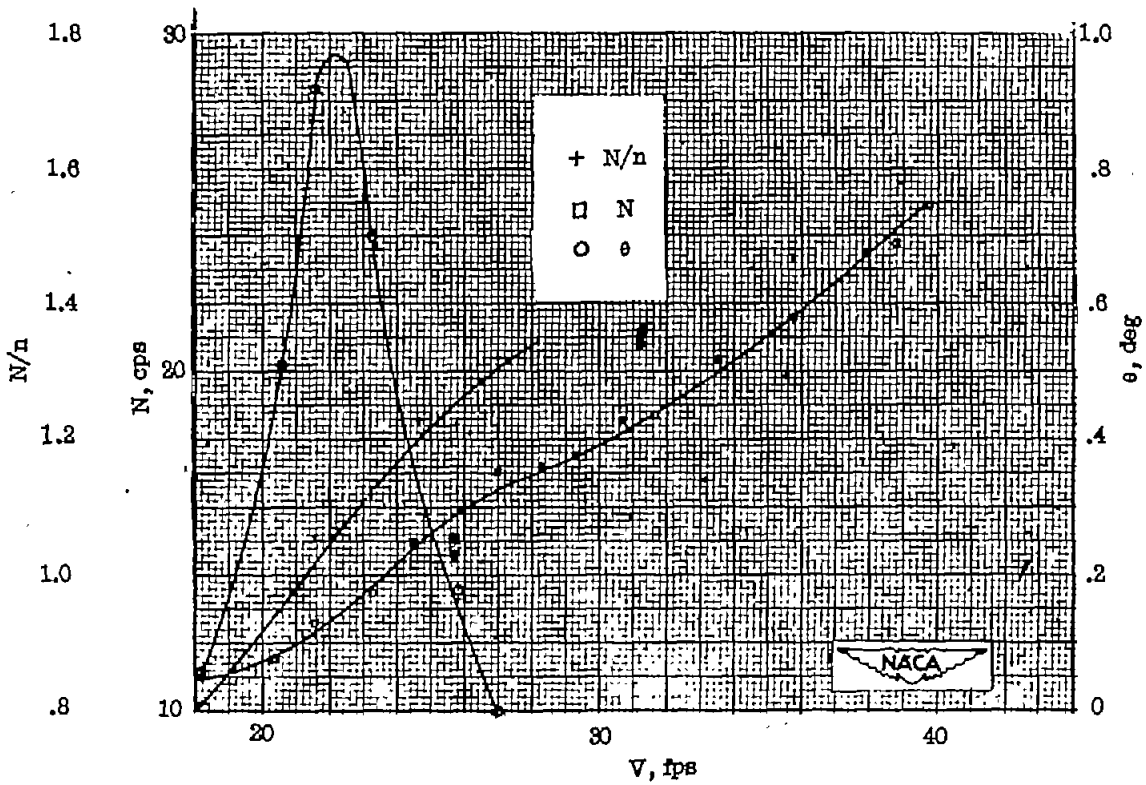

(h) $\alpha = 21^{\circ}$.

Figure 10.- Continued.

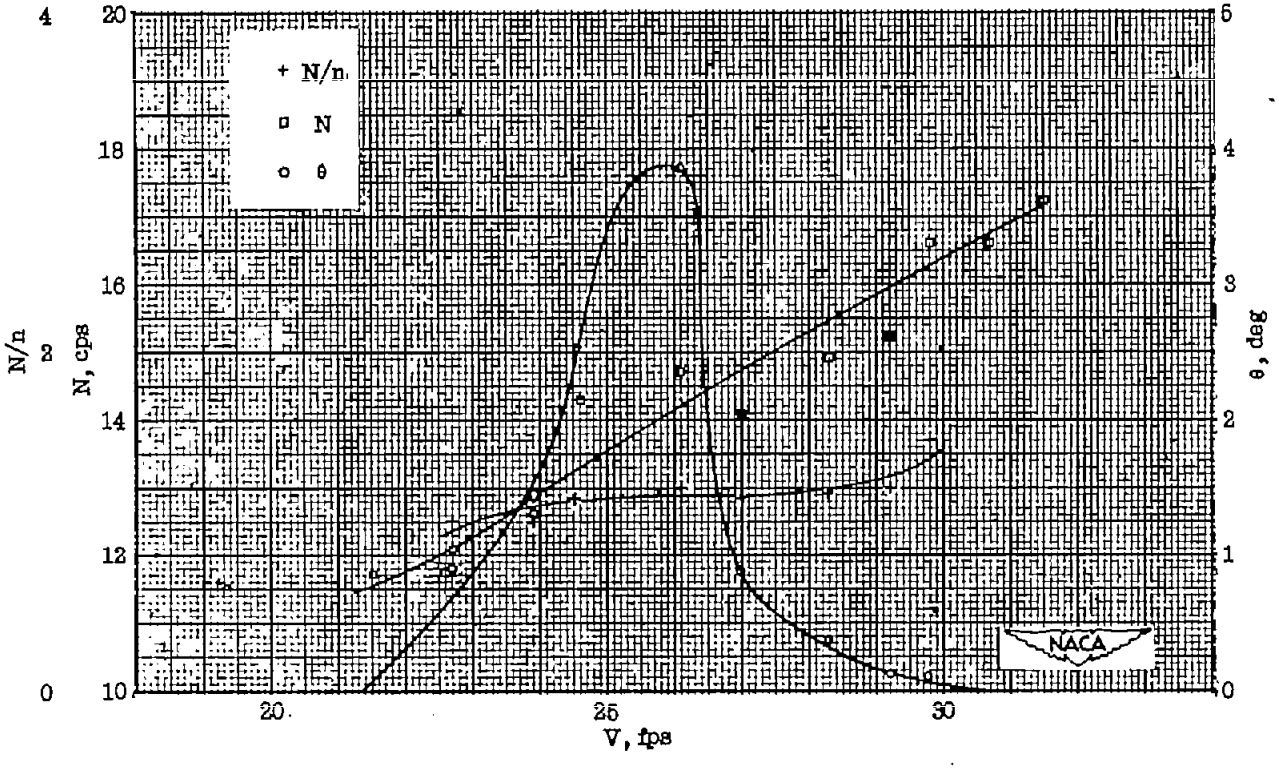

(i) $\alpha = 23^{\circ}$.

Figure 10.- Continued.

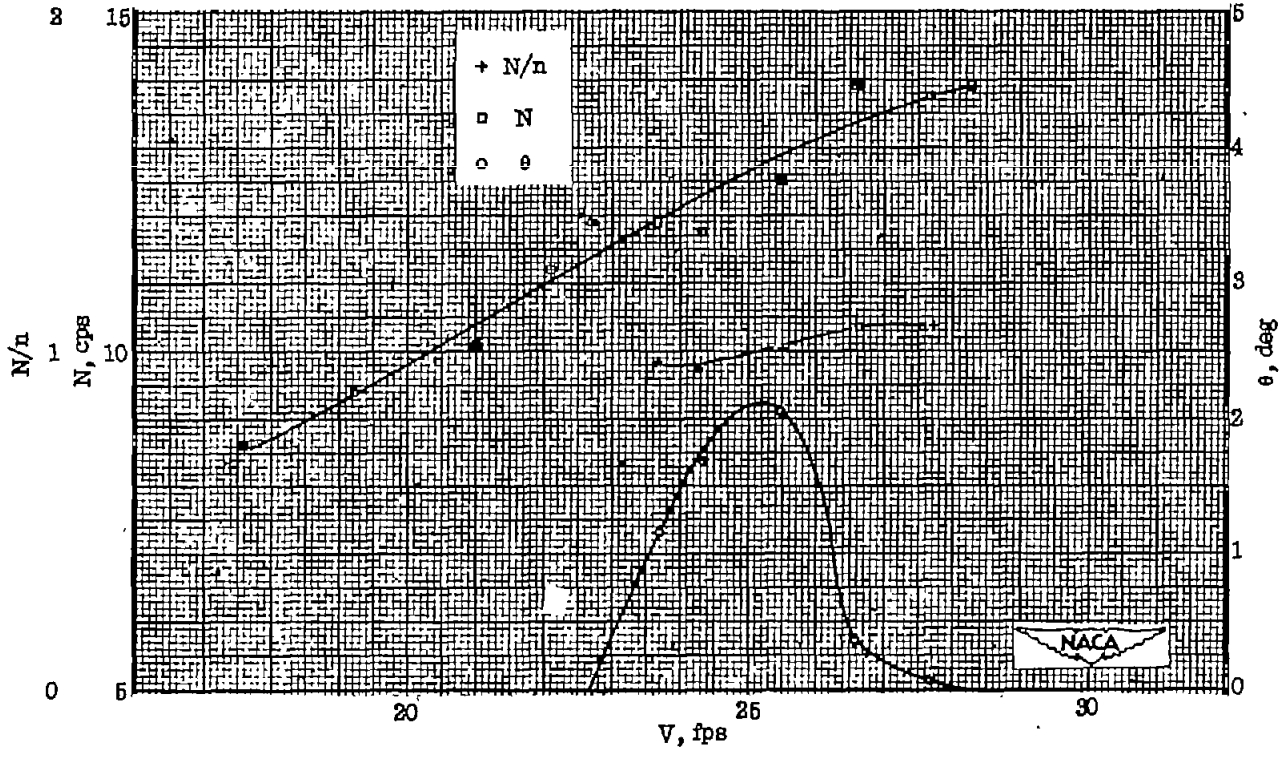

(j) $\alpha = 25^{\circ}$.

Figure 10.- Continued.

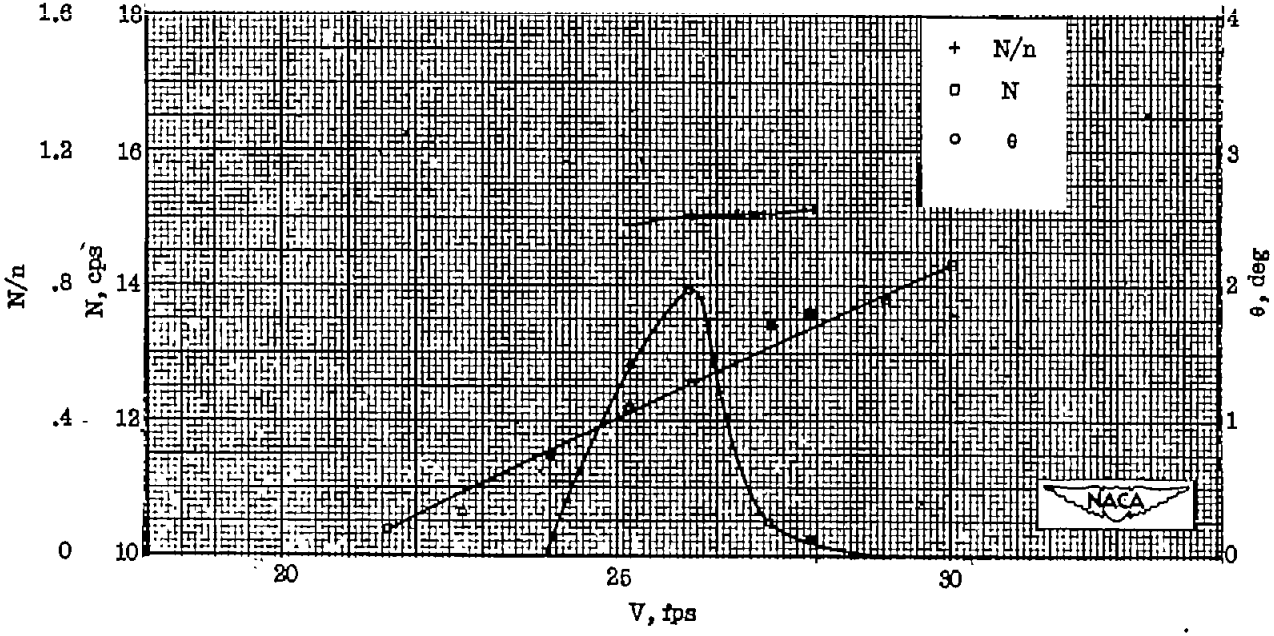

(k) $\alpha = 27^{\circ}$.

Figure 10.- Continued.

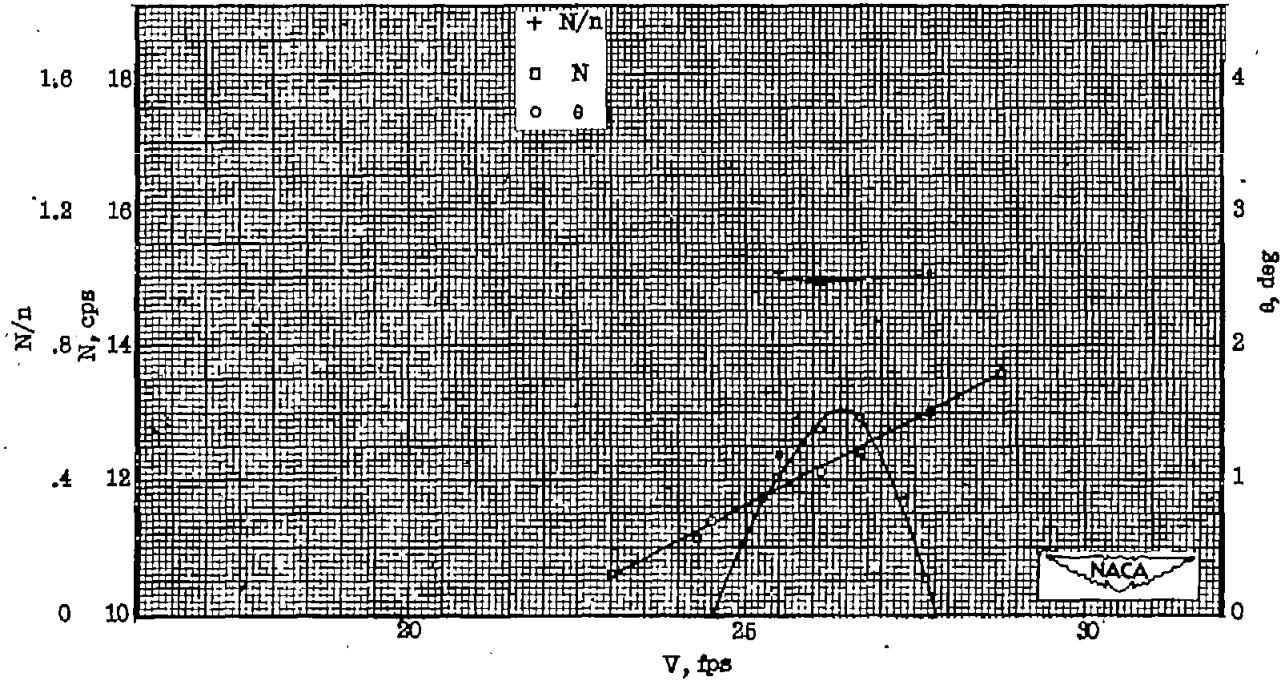

(l) $\alpha = 29^{\circ}$.

Figure 10.- Concluded.

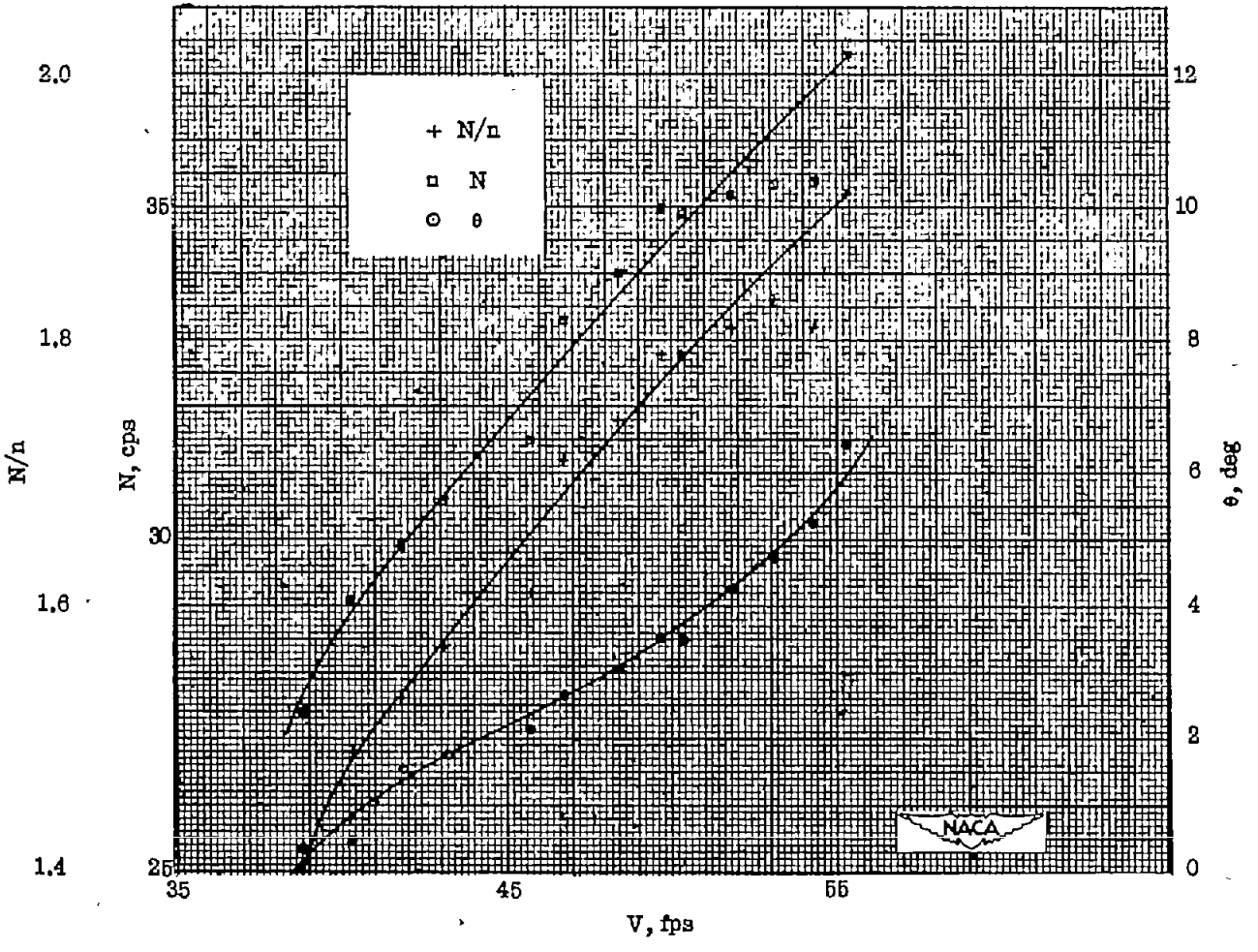

(a) $\alpha = 8^{\circ}$.

Figure 11.- Oscillation amplitude and vortex shedding frequency measurements made with suspension 2.

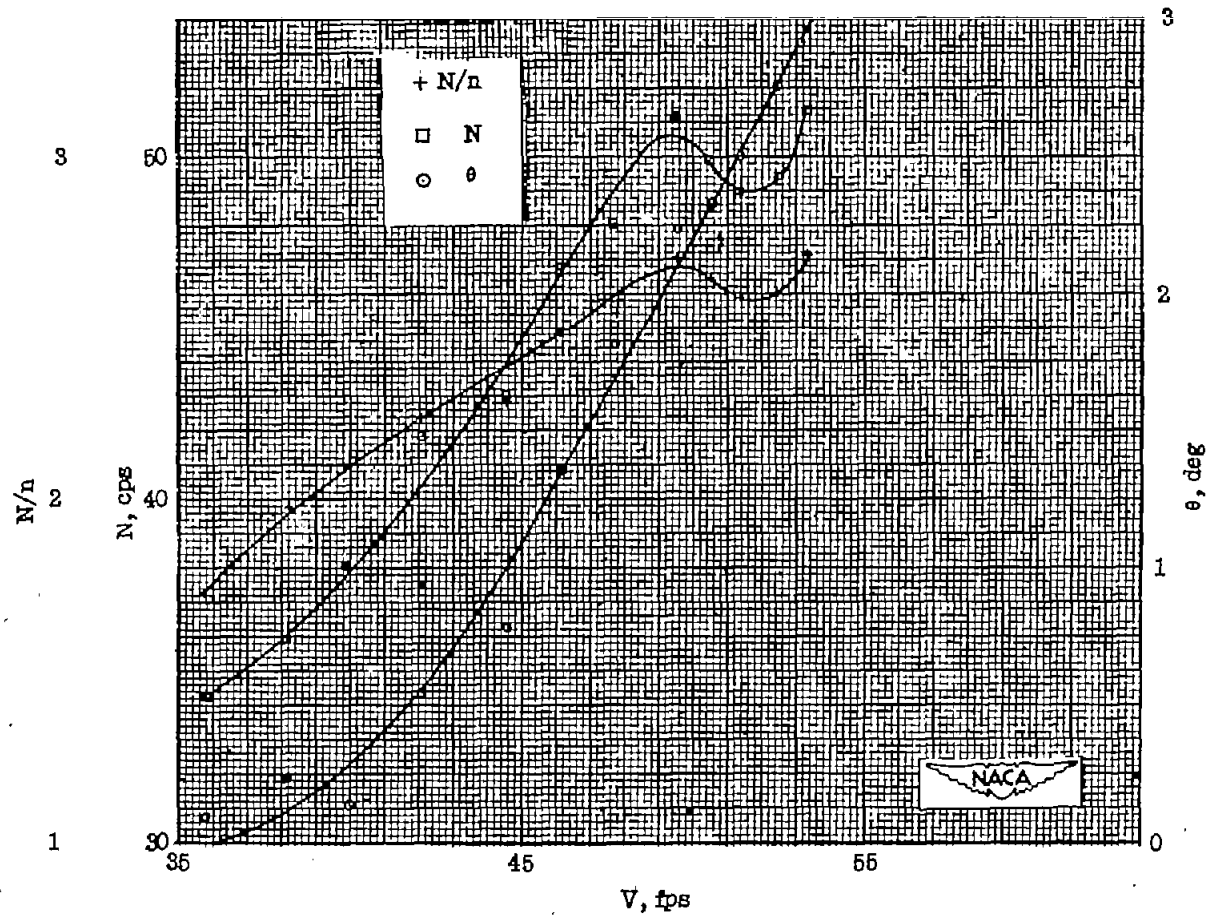

(b) $\alpha = 12^{\circ}$.

Figure 11.- Continued.

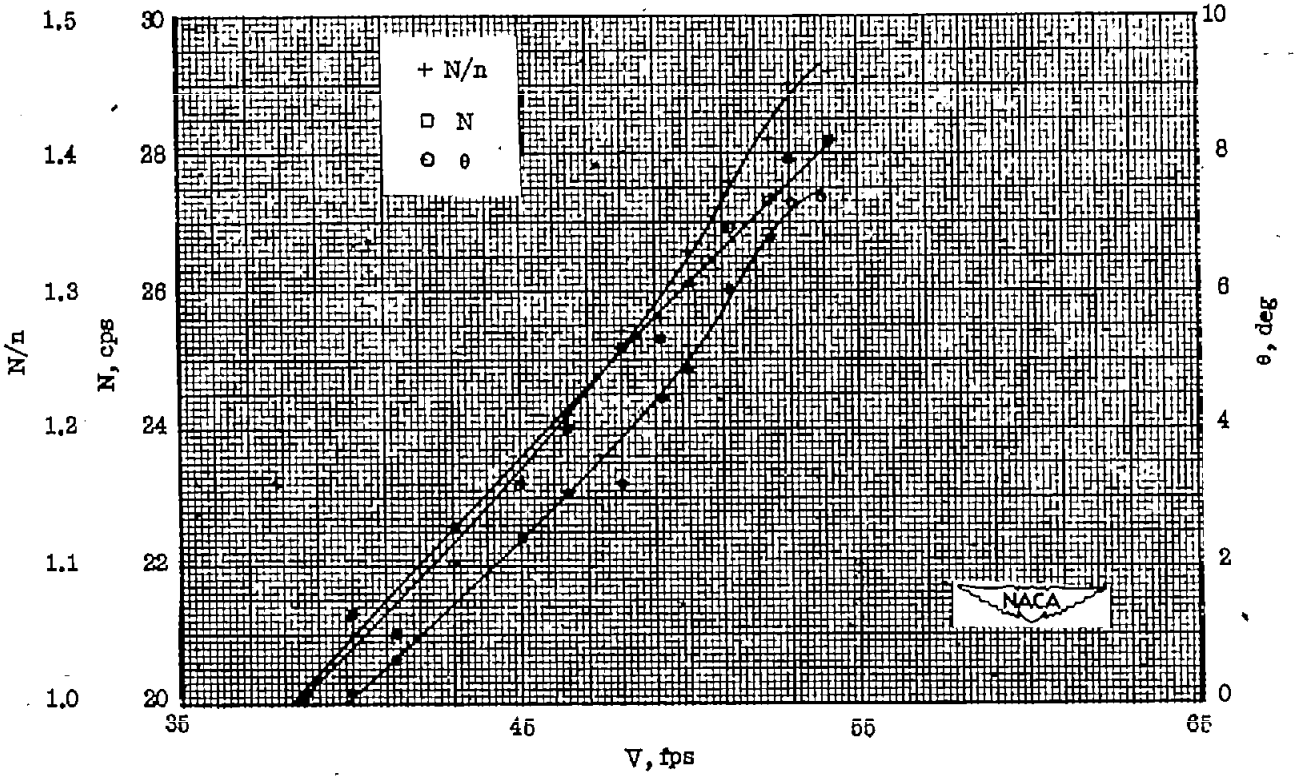

(c) $\alpha = 25^\circ$.

Figure 11.- Concluded.

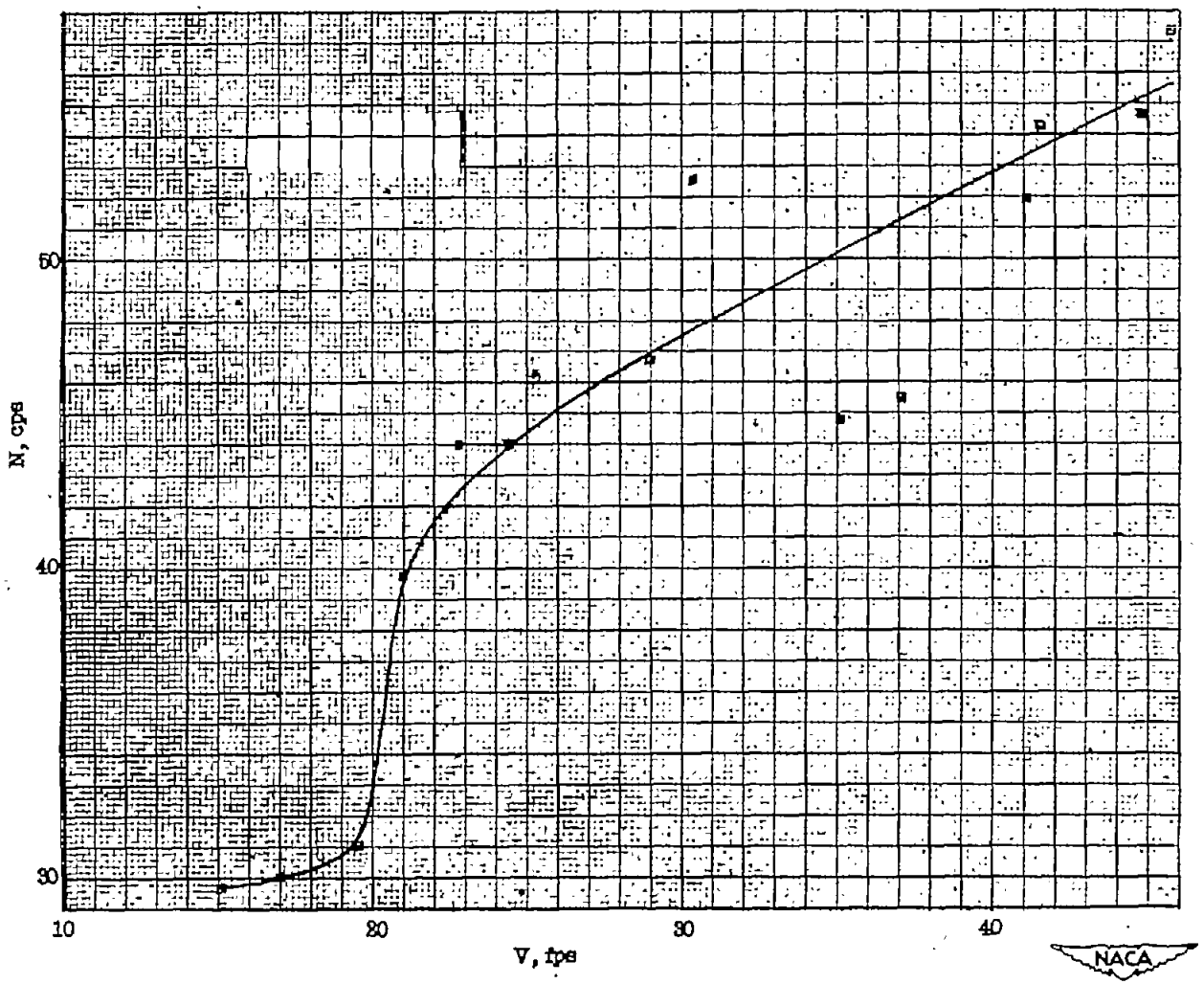

(a) $\alpha = 7^{\circ}$.

Figure 12.- Vortex shedding frequency measurements made with a hot-wire anemometer and suspension 1.

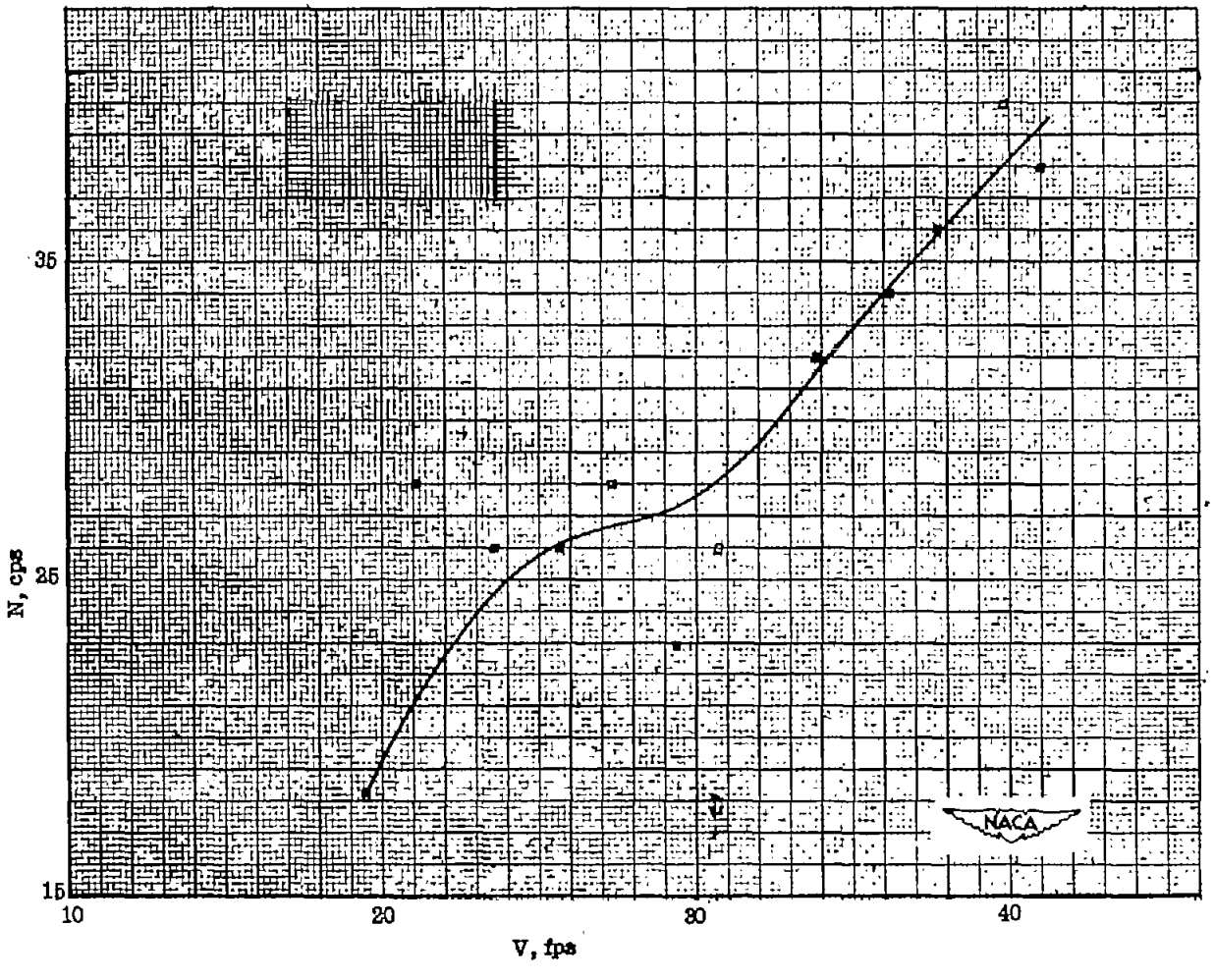

(b) $\alpha = 8^{\circ}$.

Figure 12.- Continued.

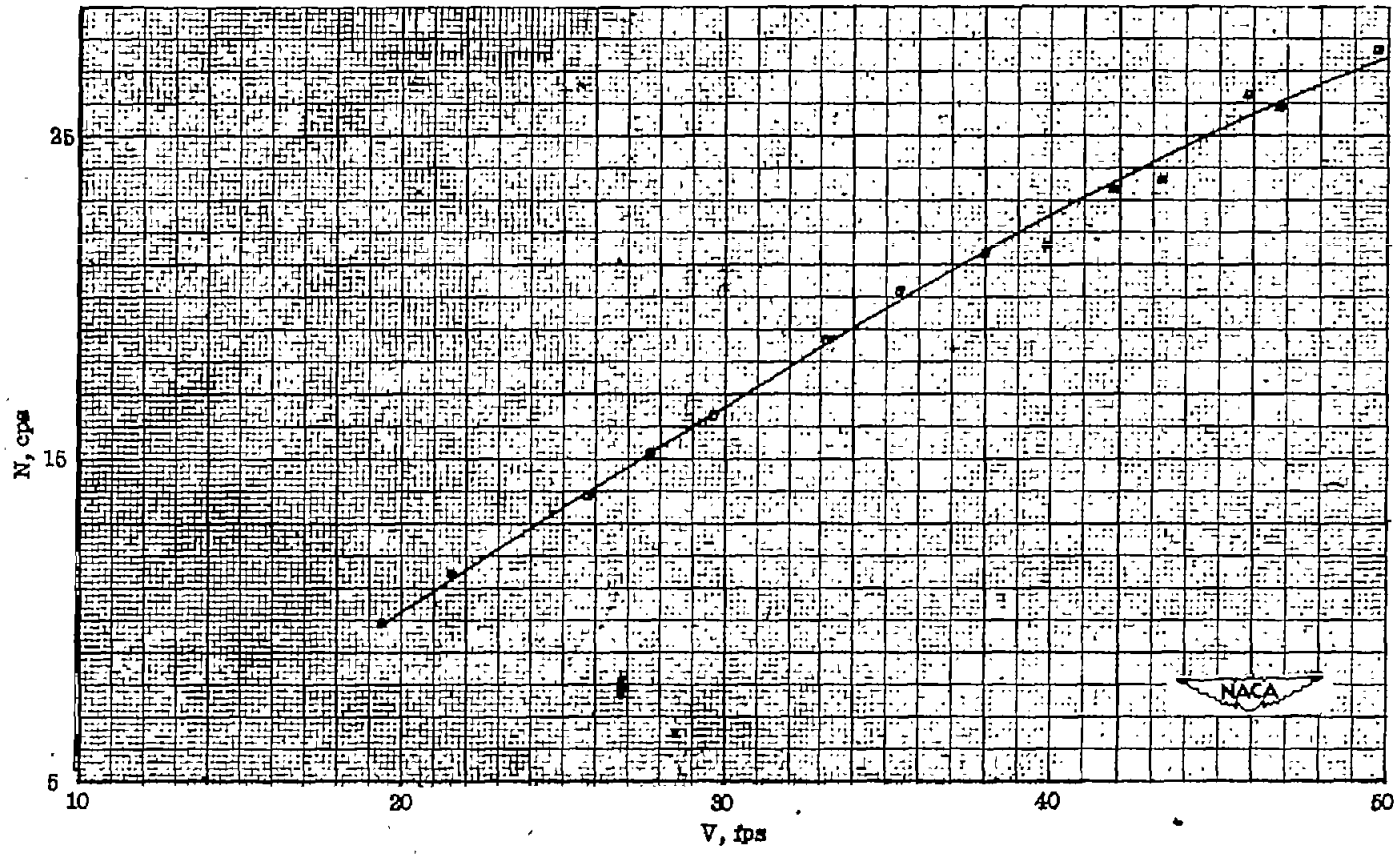

(c) $\alpha = 23^{\circ}$.

Figure 12.- Continued.

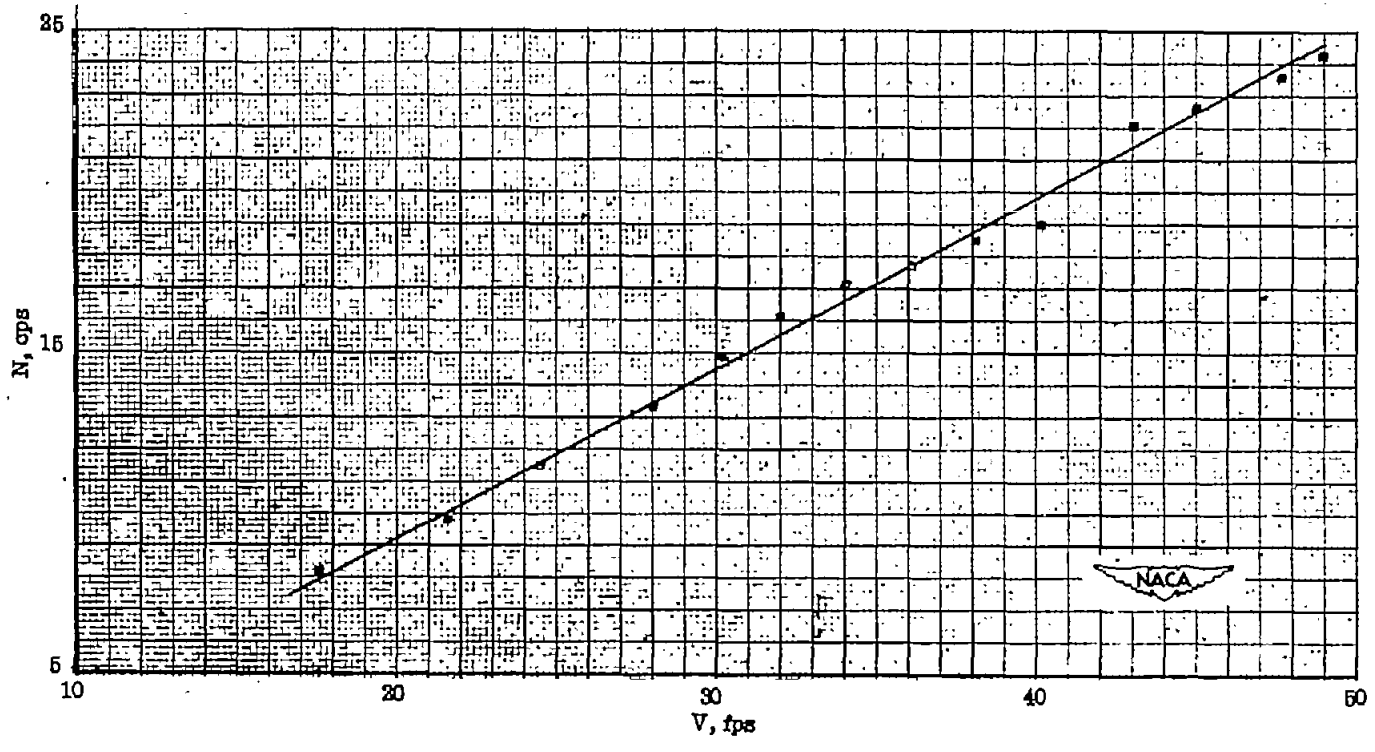

(d) $\alpha = 27^{\circ}$.

Figure 12.- Continued.

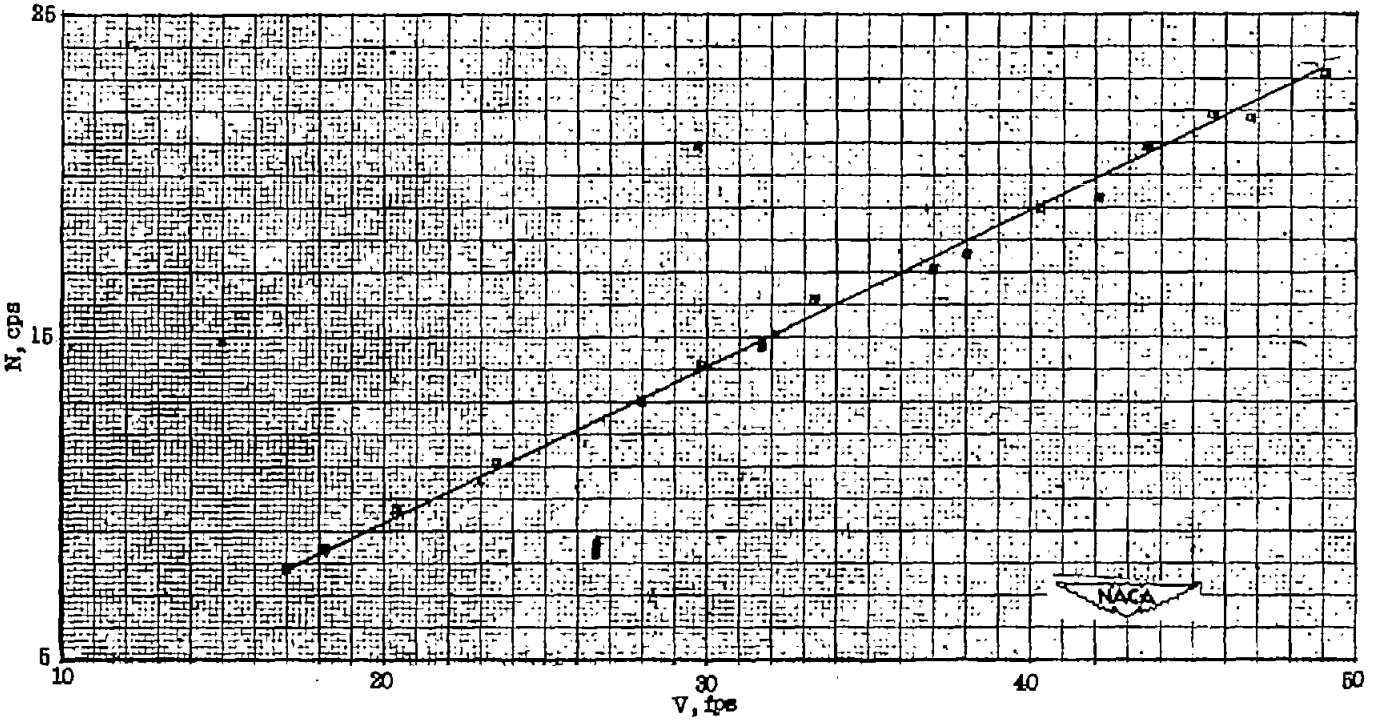

(e) $\alpha = 29^{\circ}$.

Figure 12.- Concluded.

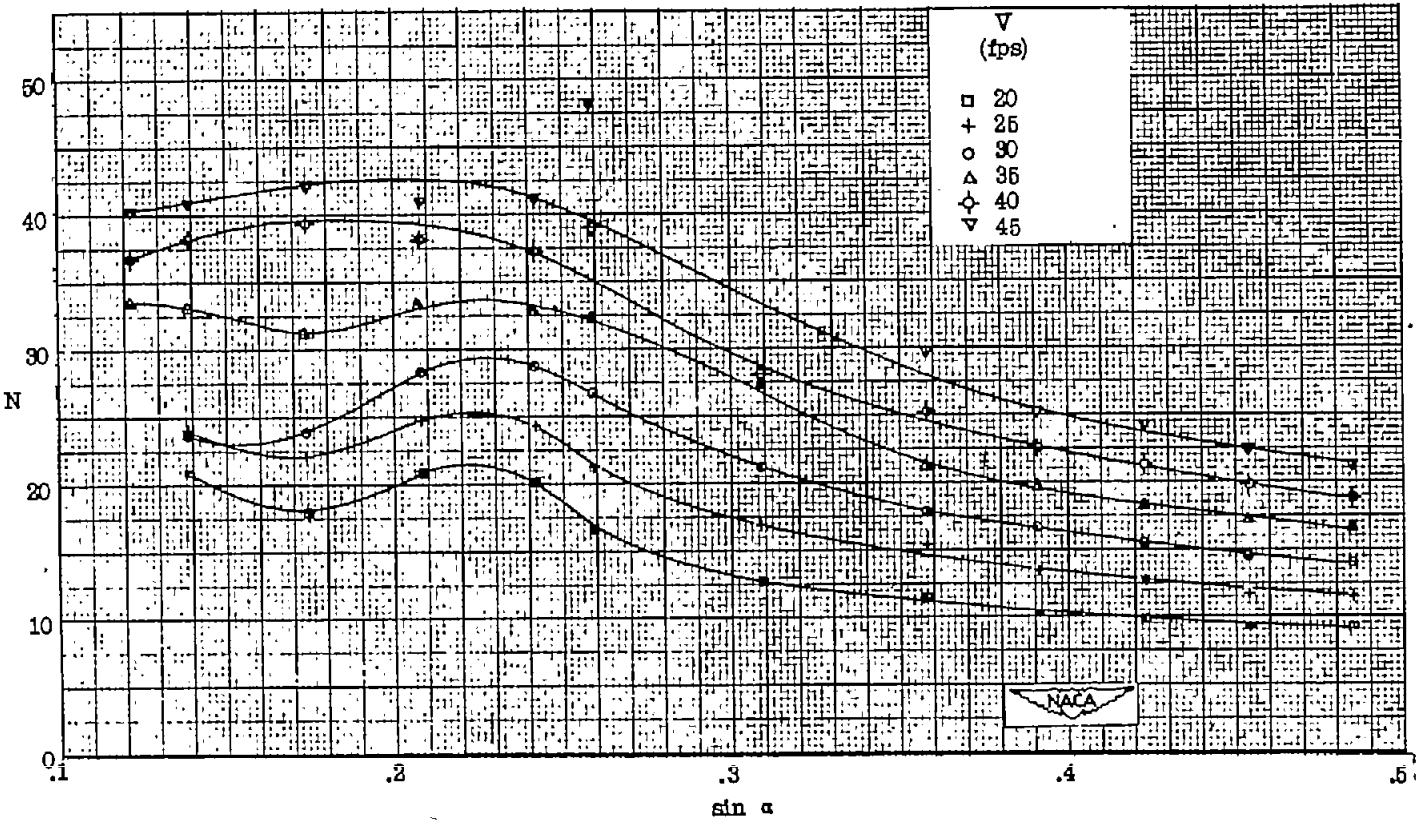

Figure 13.- Vortex shedding frequency measurements made with a hot-wire anemometer and suspension 1 plotted at various values of sin α.

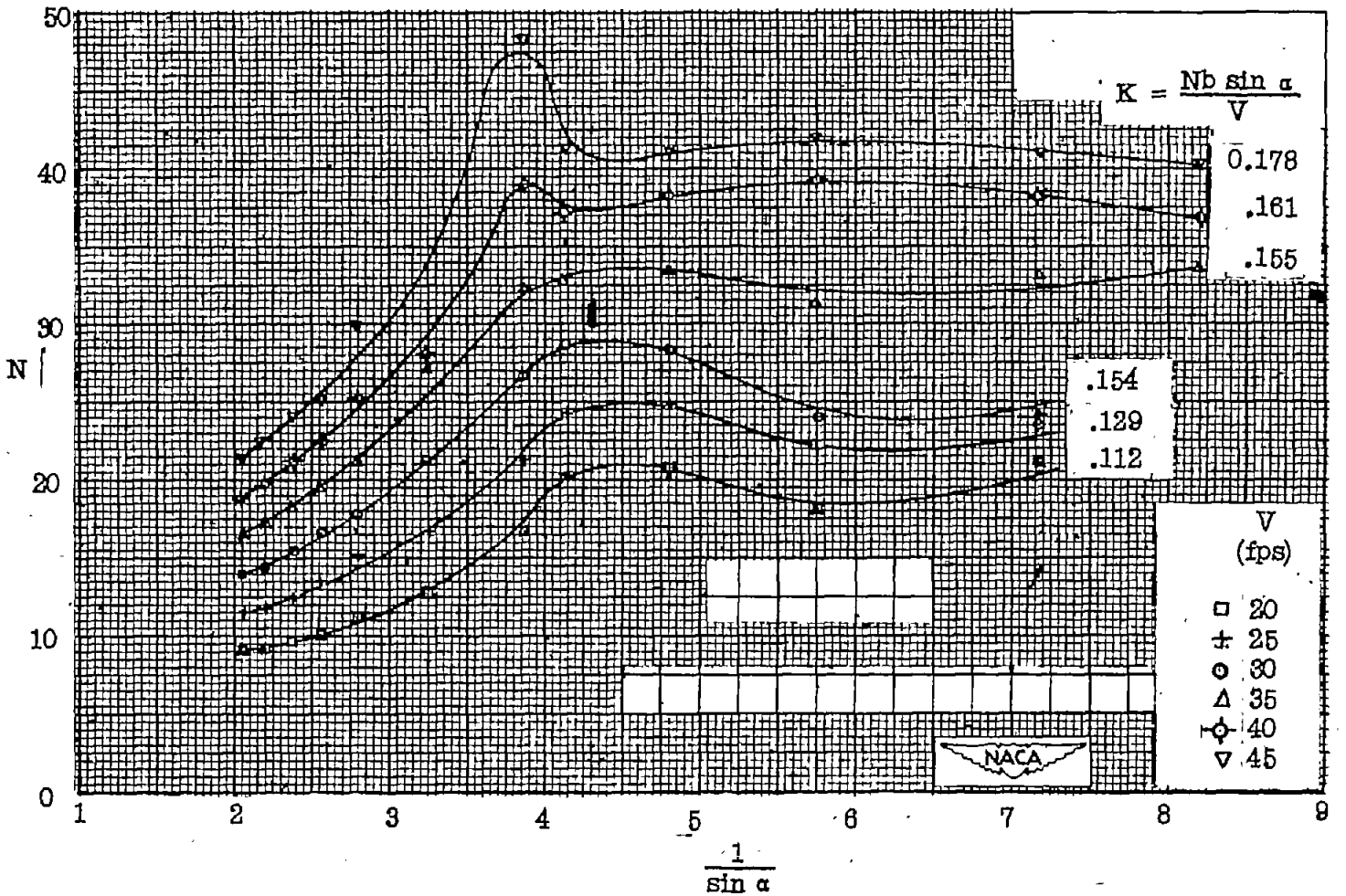

Figure 14.- Vortex shedding frequency measurements made with a hot-wire anemometer and suspension 1 plotted at various values of $1/\sin\alpha$. Value of K computed from slope of secant drawn through points at $\alpha = 29^\circ$ and $\alpha = 18^\circ$.

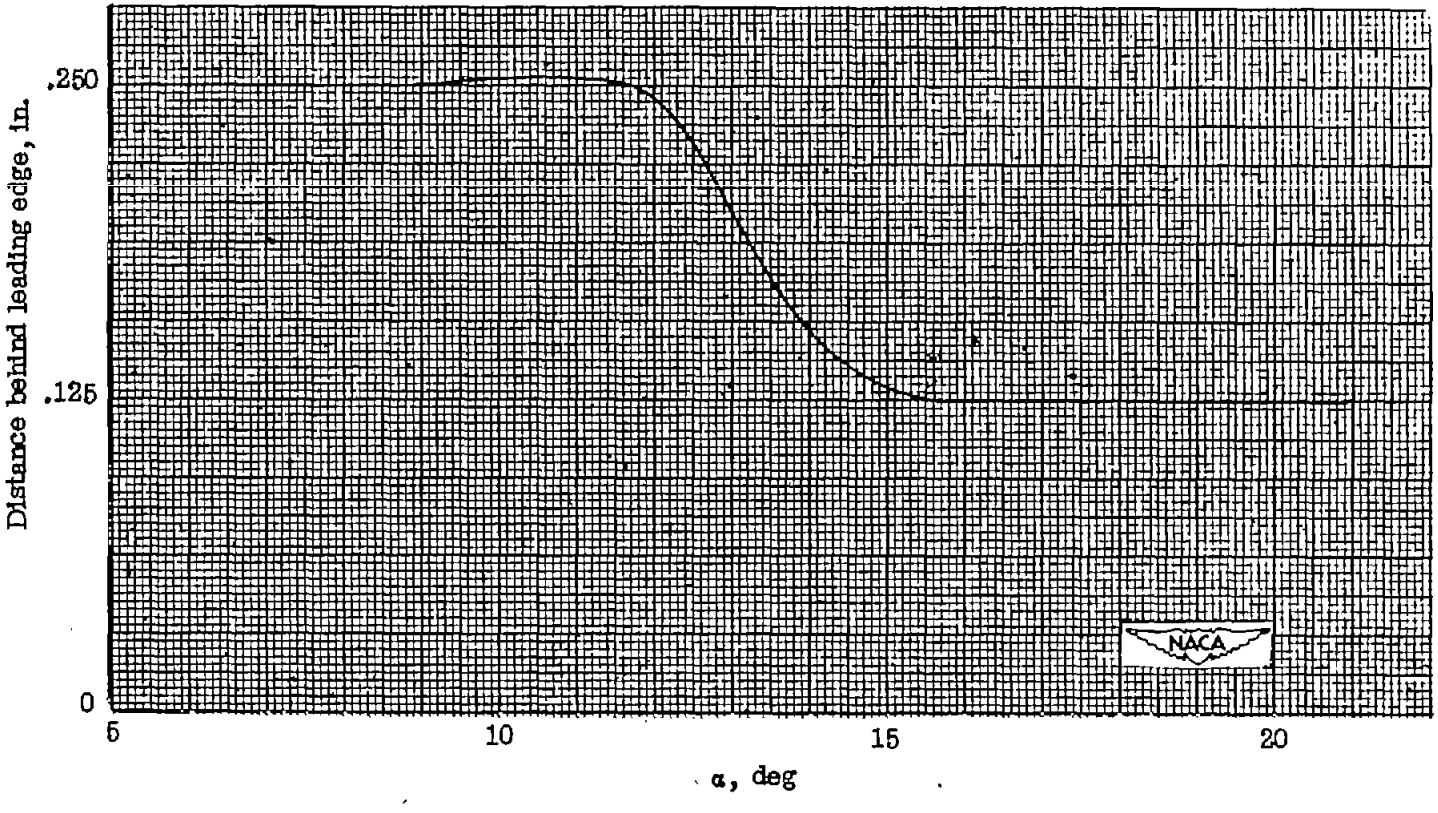

Figure 15.- Point of flow separation on upper surface found by manipulating hot-wire mounted from top of test section.

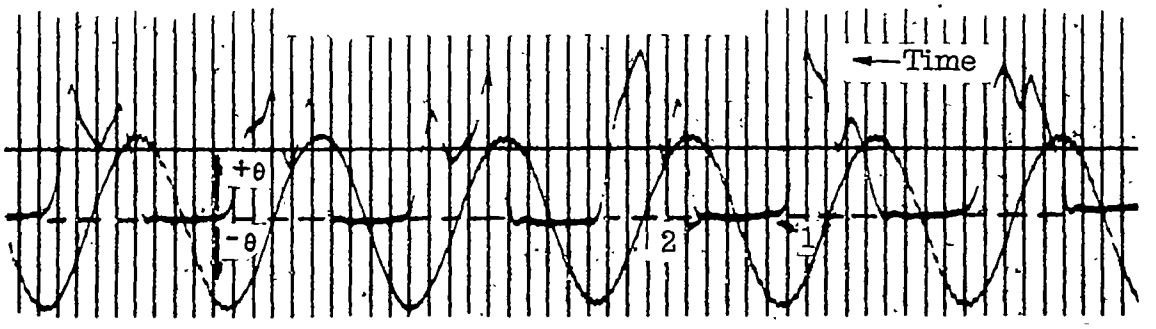

(a) Flow condition just behind leading edge. $\alpha = 8^{\circ}$, V = 53.1 feet per second, $\theta = 6.6^{\circ}$.

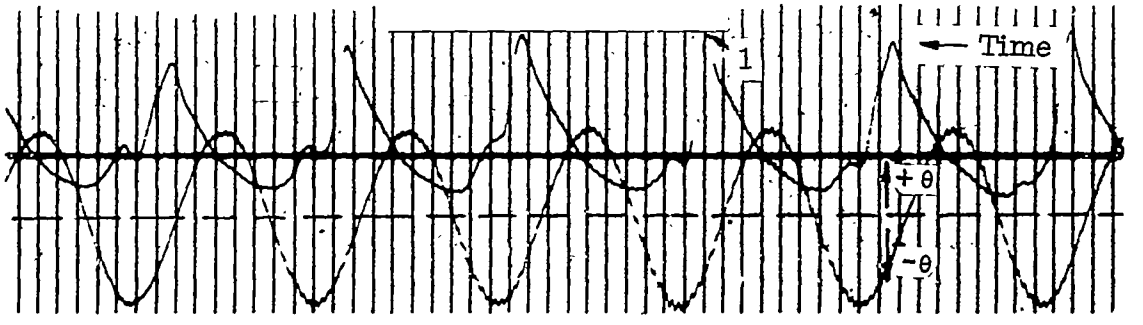

(b) Flow condition behind trailing edge. $\alpha = 8^{\circ}$, V = 53.1 feet per second, $\theta = 6.6^{\circ}$.

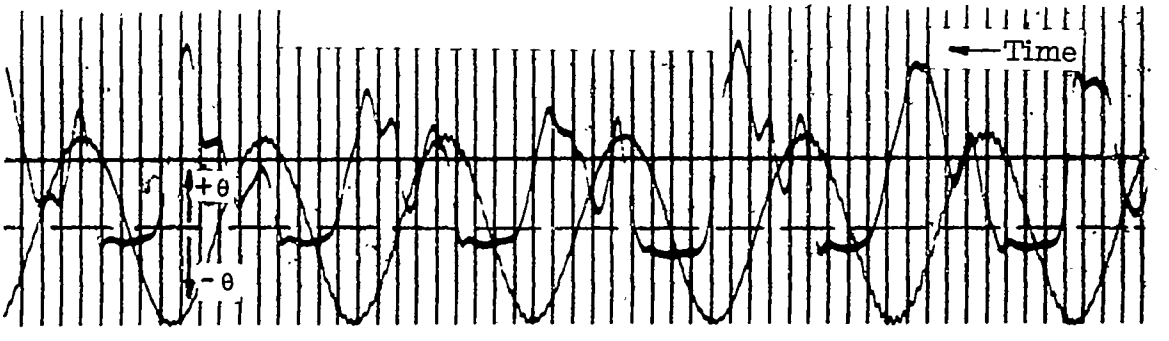

(c) Flow condition behind leading edge. $\alpha = 10^{\circ}$, V = 41.8 feet per second, $\theta = 7.0^{\circ}$.

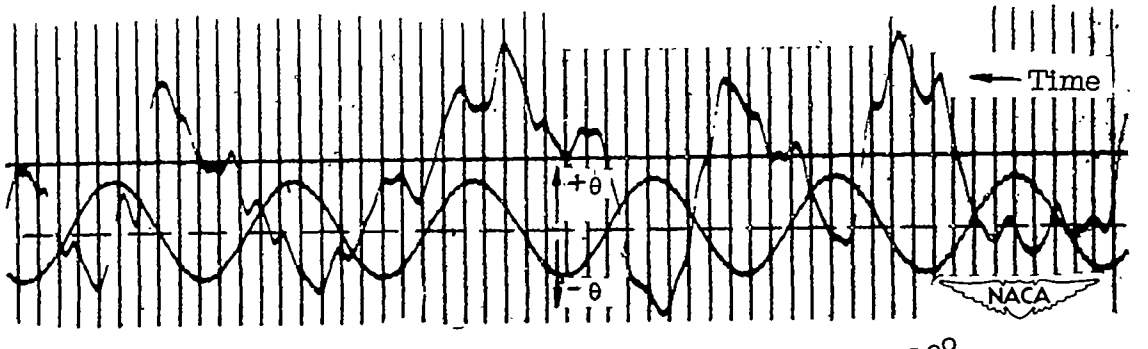

(d) Flow condition behind leading edge. $\alpha = 18^{\circ}$, V = 27.6 feet per second, $\theta = 3.6^{\circ}$.

Figure 16.- Airfoil flow conditions during oscillation.

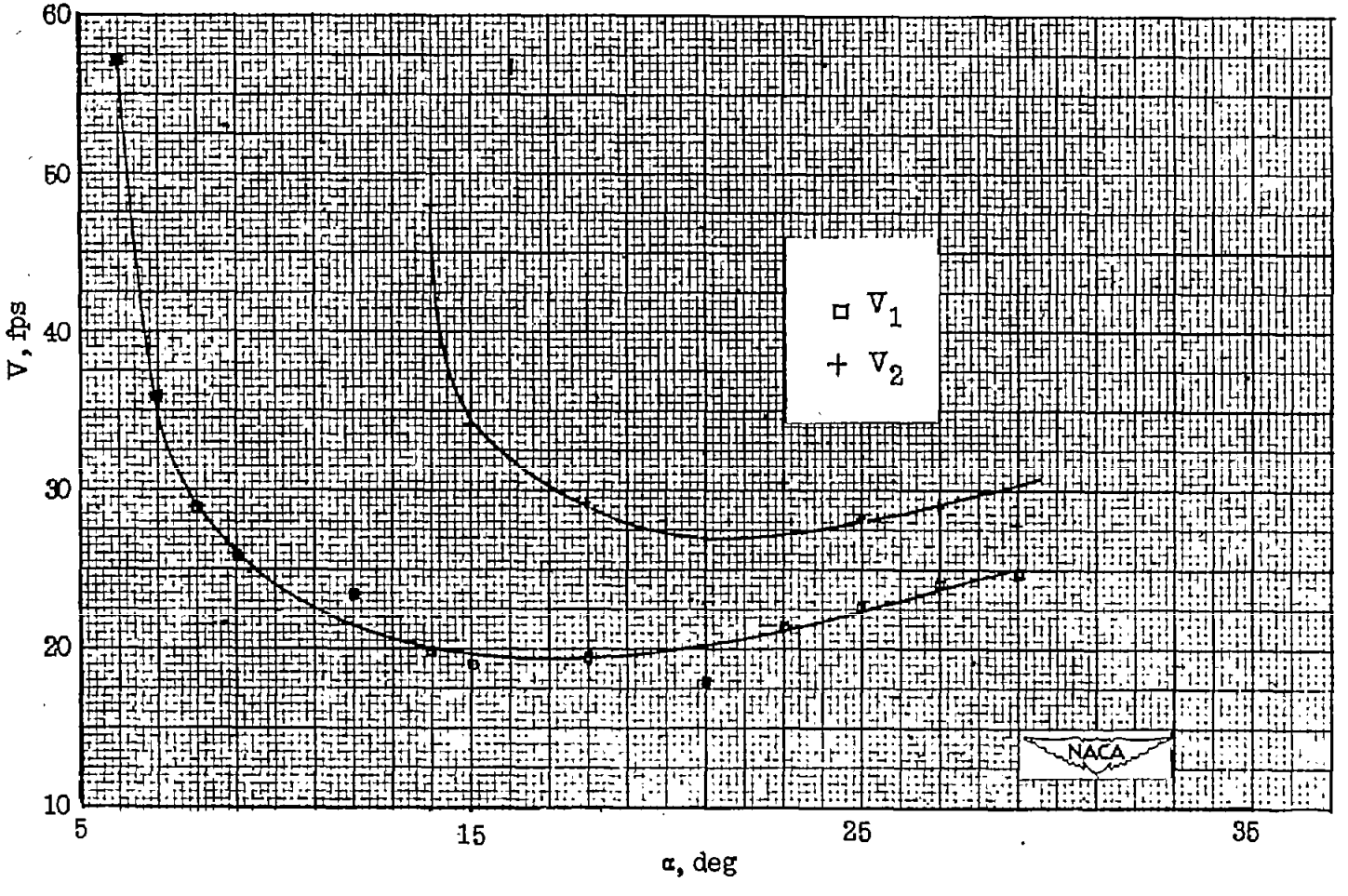

Figure 17.- Velocity range in which self-excited oscillation occurred.

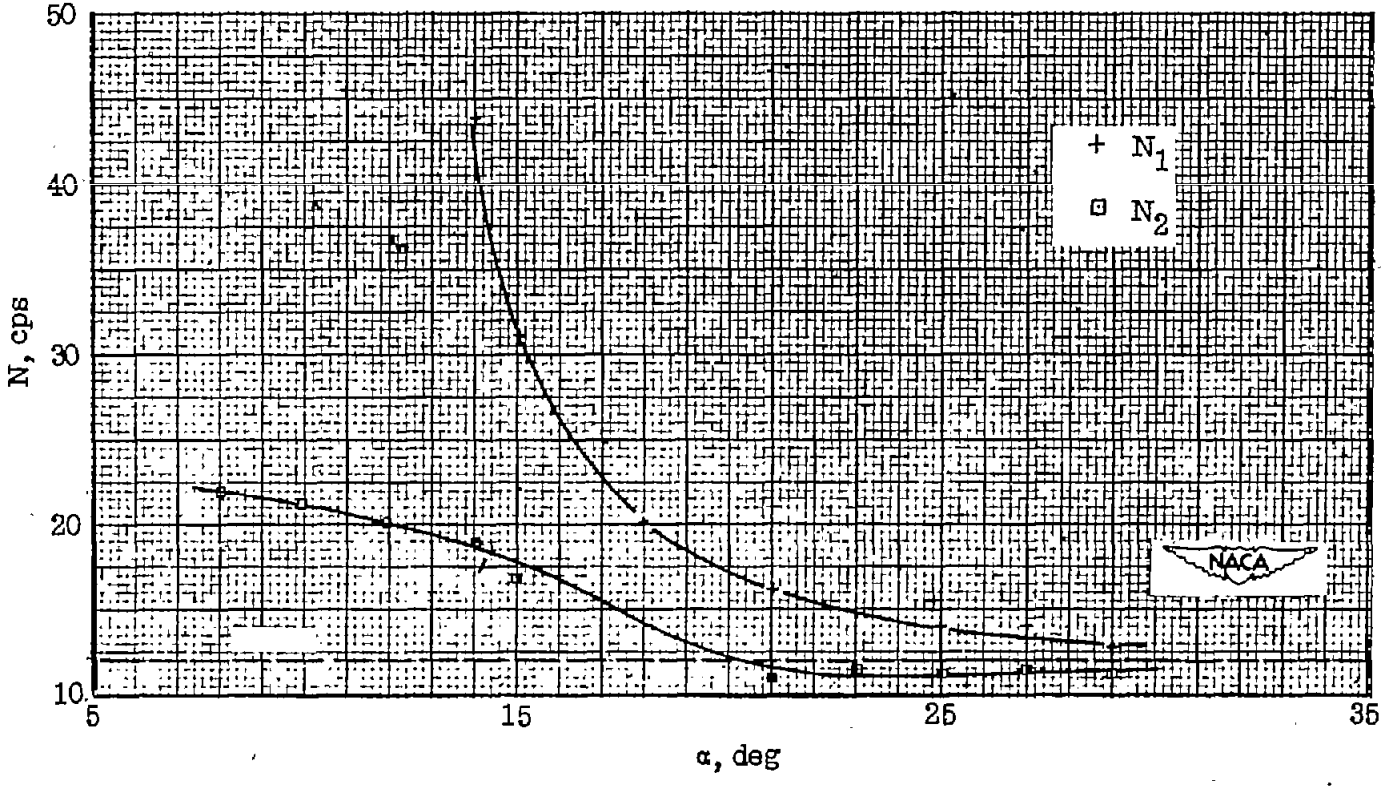

(a) Frequency of vortex shedding.

Figure 18.- Vortex frequency range in which oscillation occurred.

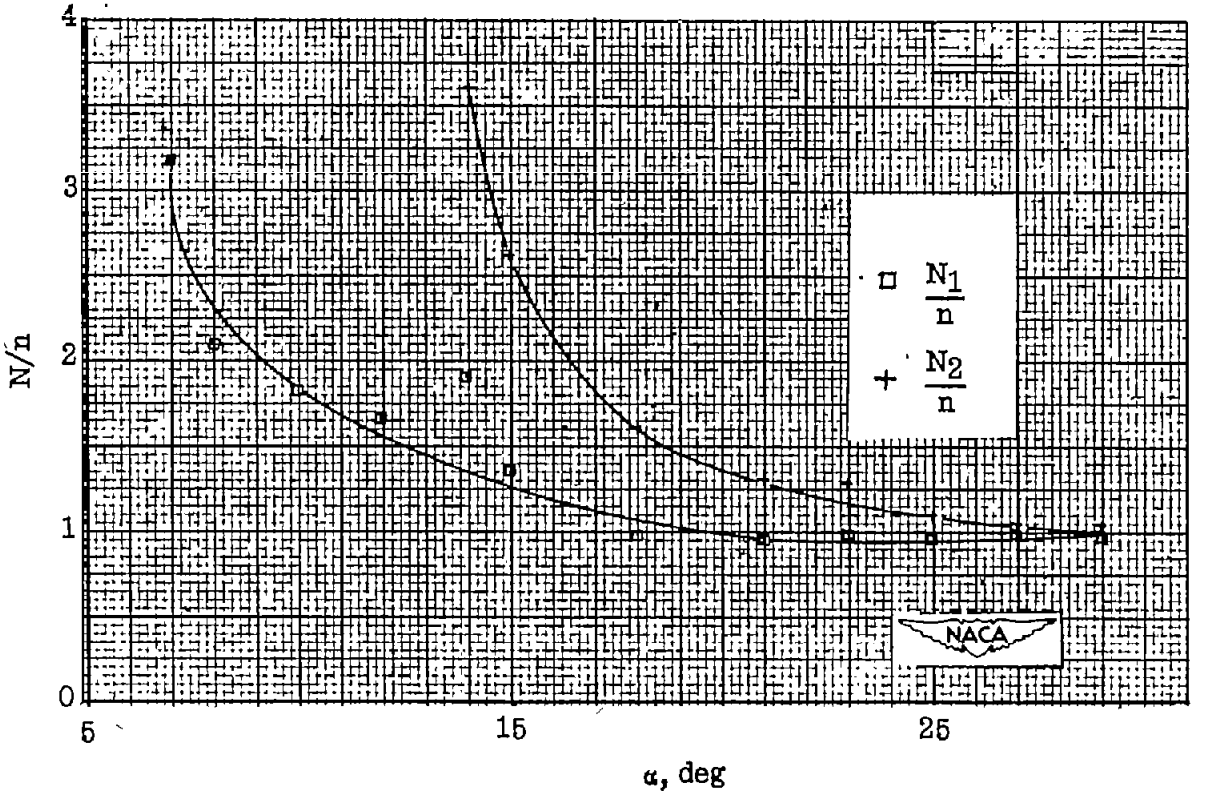

(b) Frequency of vortex shedding divided by frequency of oscillation.

Figure 18.- Concluded.

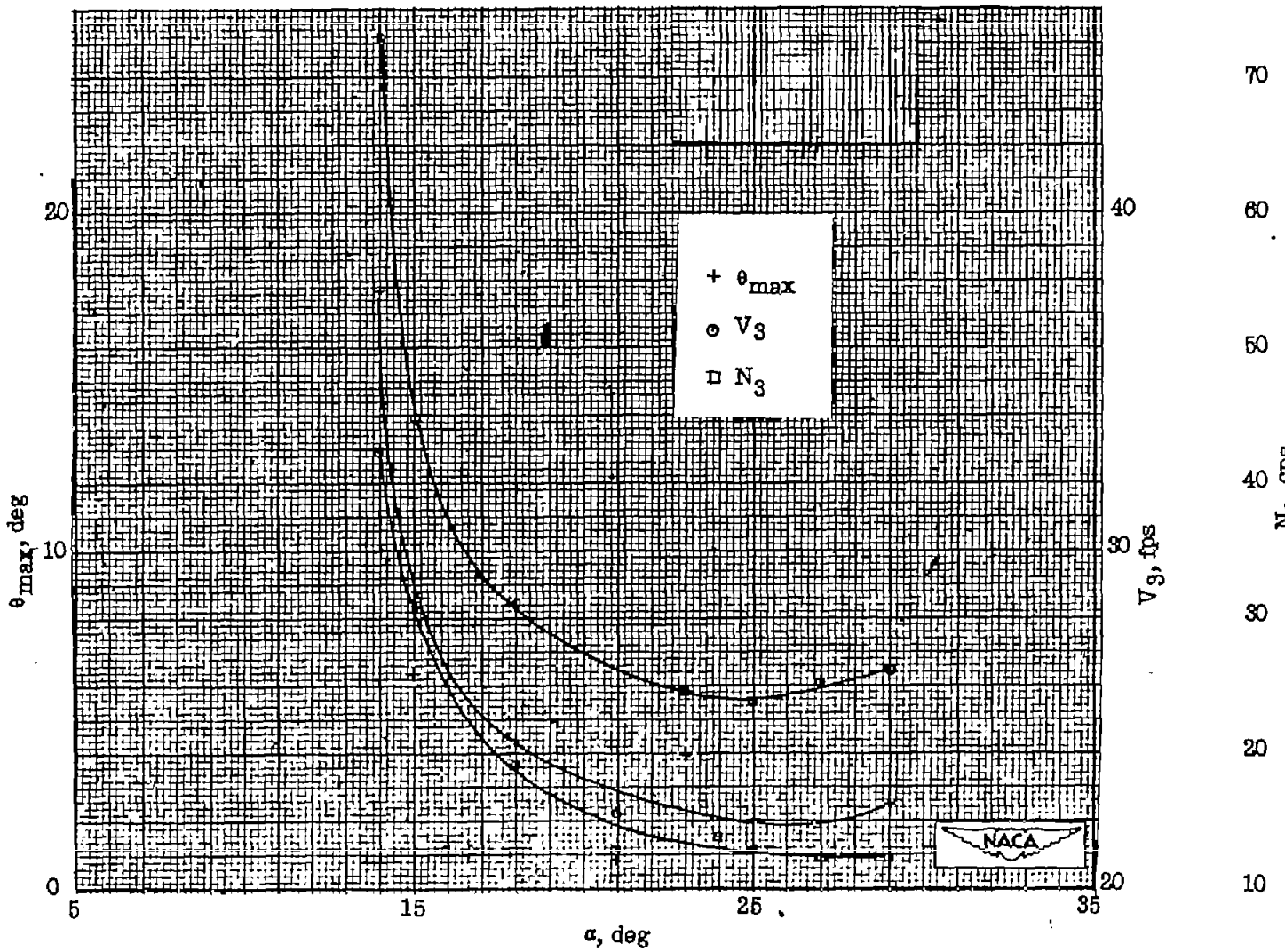

Figure 19.- Maximum amplitude of oscillation and corresponding velocity and vortex frequency for stationary airfoil.

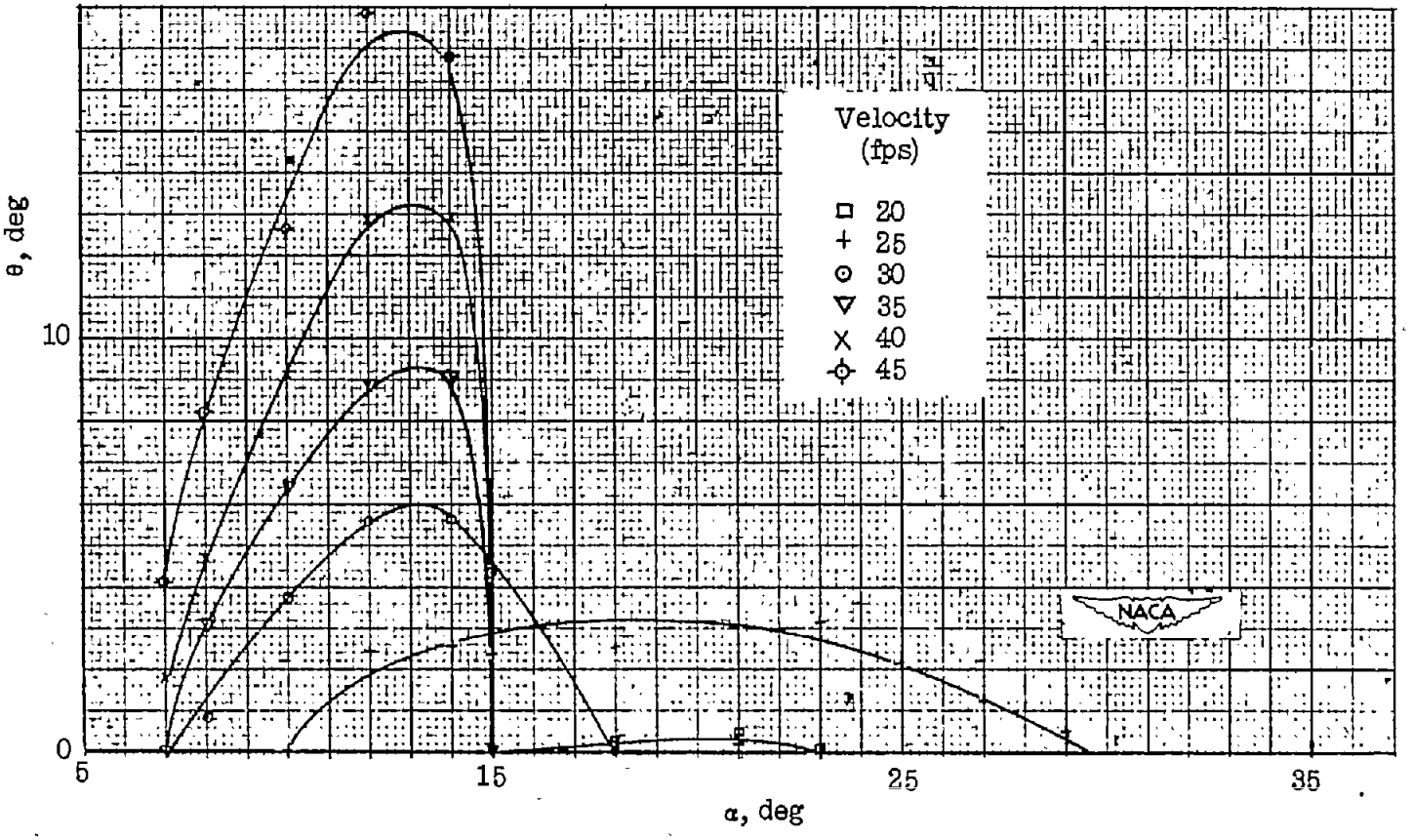

Figure 20.- Oscillation amplitude as a function of angle of attack for different velocities.

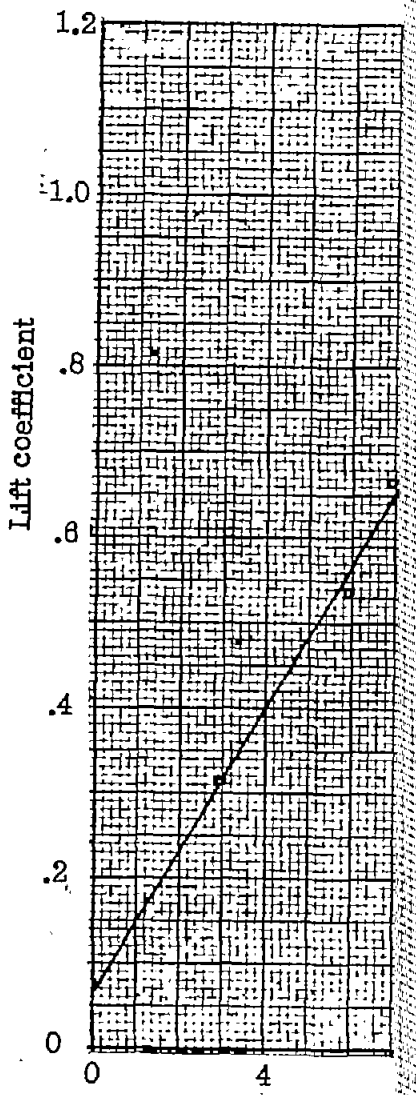

Figure 21.- Lift curve for N
9 i

NACA-Langley - 9-18-51 -1000